

**This document was prepared in conjunction with work accomplished under Contract No. DE-AC09-96SR18500 with the U. S. Department of Energy.**

**DISCLAIMER**

**This report was prepared as an account of work sponsored by an agency of the United States Government. Neither the United States Government nor any agency thereof, nor any of their employees, makes any warranty, express or implied, or assumes any legal liability or responsibility for the accuracy, completeness, or usefulness of any information, apparatus, product or process disclosed, or represents that its use would not infringe privately owned rights. Reference herein to any specific commercial product, process or service by trade name, trademark, manufacturer, or otherwise does not necessarily constitute or imply its endorsement, recommendation, or favoring by the United States Government or any agency thereof. The views and opinions of authors expressed herein do not necessarily state or reflect those of the United States Government or any agency thereof.**

**This report has been reproduced directly from the best available copy.**

**Available for sale to the public, in paper, from: U.S. Department of Commerce, National Technical Information Service, 5285 Port Royal Road, Springfield, VA 22161,  
phone: (800) 553-6847,  
fax: (703) 605-6900  
email: [orders@ntis.fedworld.gov](mailto:orders@ntis.fedworld.gov)  
online ordering: <http://www.ntis.gov/help/index.asp>**

**Available electronically at <http://www.osti.gov/bridge>  
Available for a processing fee to U.S. Department of Energy and its contractors, in paper, from: U.S. Department of Energy, Office of Scientific and Technical Information, P.O. Box 62, Oak Ridge, TN 37831-0062,  
phone: (865)576-8401,  
fax: (865)576-5728  
email: [reports@adonis.osti.gov](mailto:reports@adonis.osti.gov)**

**WSRC-TR-2003-00158**

**Revision 0**

**Keywords:** DWPF, CPC, sludge,  
SRAT, Sludge Batch 3

**Retention:** Permanent

## **Sludge Batch 3 Simulant Flowsheet Studies: Phase II SRAT/SME Results**

**C.C. Herman  
D.C. Koopman  
D.R. Best  
M.F. Williams**

**Publication Date: April 25, 2003**

**Westinghouse Savannah River Company  
Savannah River Technology Center  
Aiken, SC 29808**



**SAVANNAH RIVER SITE**

---

**PREPARED FOR THE U.S. DEPARTMENT OF ENERGY UNDER CONTRACT NO. DE-AC09-96SR18500**

**TABLE OF CONTENTS**

**1.0** EXECUTIVE SUMMARY..... 1  
**2.0** INTRODUCTION AND BACKGROUND..... 2  
**3.0** EXPERIMENTAL..... 4  
    3.1 Sludge Simulant and Slurry Preparation ..... 4  
    3.2 Procedures and Equipment Used in Testing ..... 5  
    3.3 Acid Addition Strategy ..... 6  
**4.0** ANALYTICAL..... 7  
**5.0** SRAT/SME RUN RESULTS ..... 9  
    5.1 Starting Sludge Composition ..... 9  
    5.2 SRAT and SME Processing ..... 11  
    5.3 SRAT and SME Product Characterization..... 17  
**6.0** MASS BALANCE CALCULATIONS ..... 23  
    6.1 Overall Material Balances..... 24  
    6.2 Carbon Balances ..... 24  
        6.2.1 Overall Carbon Material Balances ..... 24  
        6.2.2 Oxalate Species Material Balance ..... 26  
        6.2.3 Formate Species Material Balances ..... 27  
        6.2.4 Carbon Dioxide Species Material Balances ..... 28  
        6.2.5 Hydrogen Generation Relative to Carbon Dioxide Generation..... 30  
    6.3 SB3 Simulant Nitrogen Balances..... 31  
**7.0** CONCLUSIONS..... 34  
**8.0** PATH FORWARD ..... 34  
**9.0** REFERENCES ..... 35  
**10.0** ACKNOWLEDGMENTS ..... 36

**LIST OF TABLES**

Table 1 – Sludge Compositions (Wt% Calcined Basis)..... 5  
Table 2 - Projected Levels of Noble Metals (Sodium Oxalate Free - Dried Solids Basis) ..... 5  
Table 3 – Initial Sludge Composition: Target and Measured Comparison (Dried Solids Basis)..... 9  
Table 4 – Initial Sludge Slurry Anion Concentrations (mg/kg slurry)..... 10  
Table 5 - Physical Properties of the Initial Sludge..... 10  
Table 6 – Carbon Analyses on Starting Sludge (µg/ml) ..... 10  
Table 7– In-Process Slurry Anion Concentrations Based on Weighted Dilutions (mg/Kg) ..... 13  
Table 8 – SRAT Slurry Supernate at the End of Acid Addition (mg/L)..... 16  
Table 9 – SRAT and SME Product Anion Concentration (mg/kg)..... 17  
Table 10 – Destruction of Nitrate, Formate, and Oxalate – SRAT Receipt Relative to SRAT Product and SRAT Product Relative to SME Product ..... 18  
Table 11 – SRAT and SME Product Results (Calcined Solids Wt%) ..... 19  
Table 12 – Filtered SRAT and SME Product Supernate (mg/L) ..... 20  
Table 13 - Physical Property Data on SRAT and SME Products ..... 20  
Table 14 – Carbon Analyses on the SME Products (µg/ml) ..... 21  
Table 15 – Analyses of FAVC, MWWT, and SMECT Samples ..... 22  
Table 16 – “Carbon In” Scaled to 6000 Gallons at 18 wt. % Total Solids (lbs) ..... 25

Table 17 – “Carbon Out” Scaled to 6000 Gallons at 18 wt. % Total Solids (lbs)..... 26  
Table 18 - Closure of the Overall Carbon Balance ..... 26  
Table 19 - Oxalate Balance Scaled to 6000 Gallons at 18 wt. % Total Solids..... 27  
Table 20 - Formate Balance Scaled to 6000 Gallons at 18 wt. % Total Solids..... 27  
Table 21 - Gross Formate Loss from Consumption Reactions ..... 28  
Table 22 - CO<sub>2</sub> Balance Scaled to 6000 Gallons at 18 wt. % Total Solids ..... 29  
Table 23 - Carbon Dioxide Mass Evolved in SME Cycle Phases at DWPF Scale (lbs)..... 30  
Table 24 - Hydrogen Mass Evolved at DWPF Scale (lbs)..... 30  
Table 25 - Carbon Dioxide Generation Associated with Hydrogen Generation (lbs)..... 31  
Table 26 - Nitrate Balance Scaled to 6000 Gallons at 18 wt. % Total Solids ..... 31  
Table 27 - Nitrous Oxide Mass Evolved at DWPF Scale (lbs)..... 32  
Table 28 - Calculated SRAT Acid Demand for Nitrite Destruction ..... 33  
Table 29 - Mean Acid Requirement for Nitrite Destruction vs. Oxalate Content..... 33  
  
[Table A - 1: SRAT/SME Run Parameters](#) ..... 38  
[Table A - 2: SRAT/SME Operating Data and Mass Balance](#) ..... 39

**LIST OF FIGURES**

Figure 1 – Schematic of SRAT Equipment Set-Up ..... 6  
Figure 2 – pH Plots during SRAT/SME Processing ..... 12  
Figure 3 – pH Plots during SRAT Processing for Decants 5 and 9 in Phases I and II..... 12  
Figure 4 – GC Data from Run SB3A-8..... 14  
Figure 5 – GC Data from Run SB3A-9..... 15  
Figure 6 – Hydrogen Generation on a DWPF Scale ..... 16

## 1.0 EXECUTIVE SUMMARY

The Savannah River Technology Center (SRTC) - Immobilization Technology Section (ITS) was requested to perform simulant bench-scale flowsheet studies to qualify Sludge Batch 3 (SB3), the next sludge batch to be processed at the Defense Waste Processing Facility (DWPF). Simulant flowsheet runs have been performed for every sludge batch that has been qualified for DWPF processing to date. SB3 will consist primarily of Tank 7 sludge, but will also contain transfers from other tanks and processes at the SRS and other materials not considered typical for DWPF processing. Projections also indicate that SB3 may contain higher than previously observed levels of noble metals. Over the last year, SRTC has focused significant effort on studies to understand the behavior of SB3 and to evaluate any necessary process changes.

For SB3, the simulant flowsheet runs for the chemical process cell were divided into two phases and were based on the projected composition for SB3. The first phase used nominal decant composition information obtained from High Level Waste – Program Development and Integration and consisted of four runs. All of the SB3 simulants contained 10% of the projected noble metal concentrations. The primary intention of the runs was to understand chemical process cell behavior at the different decant scenarios, but the runs also helped refine the acid addition equation necessary for SB3. The Phase I results have already been documented in WSRC-TR-2003-00088.[1] Other flowsheet run results, the revised acid addition equation, and the proposed Reduction/Oxidation (REDOX) correlation are also documented elsewhere.[4,5,9,18] The Phase II runs were initiated in February 2003 and focused on the baseline nominal decants with nominal projected noble metals and excessive acid addition amounts. The second phase used excess acid to attempt to bound the amount of acid that could be processed with the decant scenarios for SB3.

Two Sludge Receipt and Adjustment Tank (SRAT) cycles were combined with Slurry Mix Evaporator (SME) cycles to complete the second phase of the simulant flowsheet runs with SB3 simulant. The compositions evaluated included: Decant 5 with ~69% remaining sodium oxalate (Run SB3A-8) and Decant 9 with ~40% remaining sodium oxalate (Run SB3A-9). Decant oxide and anion compositions utilized were defined by High Level Waste – Program Development and Integration and represent a combination of washing/decant scenarios for SB3. The sludges were prepared from the same SB3 starting simulant used in the Phase I testing and were representative of the targeted compositions. Both SRAT runs were performed at ~25% higher acid addition levels than the Phase I runs. Frit 202 at a 35 wt% waste loading, on an oxide basis, was used for both SME cycles. Frit 202 was used because an operating window was available and the frit was also readily available. The waste loading selected was the midpoint of the waste loading operating window.

The runs easily met the DWPF SRAT product nitrite destruction acceptability criteria of <1000 ppm. Hydrogen generation, however, exceeded the DWPF SRAT hydrogen limit (0.65 lbs/hr) and was 1.4 lbs/hr in the Decant 5 run (SB3A-8). On the other hand, the Decant 9 run did not generate hydrogen above the SRAT hydrogen limit, but approached the limit with a rate of 0.42 lbs/hr. Hydrogen continued to be generated during the SME cycle, but the SME limit (0.223 lbs/hr) was not exceeded. The highest peak in the SME occurred in the Decant 9 run (0.092 lbs/hr).

The following insights into SRAT/SME processing were gained:

- No foaming or processing issues such as air entrainment were identified using nominally 2.5 liters of SRAT slurry. Visually, the sludge slurry appeared to be very thin, and no problems with mixing or heating were encountered.
- The minimum SRAT pH was obtained at the end of acid addition, and was below 4.6 for both runs. By the end of SRAT processing, the pH was >7. The slurry pH oscillated during the decontamination canister additions/dewaters and the frit addition/concentration part of the SME cycle. By the end of the SME cycle, the pH had risen to <8.
- At the tested level of noble metals, excessive hydrogen can be generated when sufficient excess acid is added. By design, excess acid was tested for both decant scenarios. For Decant 5, the acid addition amount, 1.53 moles H<sup>+</sup>/liter of slurry with 0.994 moles/liter as formic acid, created excessive hydrogen generation. For Decant 9, the acid addition amount, 1.30 moles H<sup>+</sup>/liter of slurry with 0.904 moles/liter as formic acid, presented a possible upper bound. The acid split used was calculated from an interim version of the SB3 redox equation and was based on assumed formate, oxalate, and nitrate destruction, which were under-predicted. Knowing the relative destruction of these anions with greater certainty may have resulted in a shift in the split of the acids while still using the same total acid, which in turn could have affected the amount of hydrogen generated.

- Based on the analytical data for the SRAT and SME products, significant amounts of formate were destroyed during processing. SRAT formate destruction was ~19 to 37%, while an additional ~34 to 52% was destroyed during the SME. The amounts of oxalate destroyed during processing were different between the two runs. SRAT oxalate destruction was more significant in the Decant 5 run (SB3A1-8) with ~21% destroyed, while the Decant 9 run (SB3A-9) oxalate destruction was negligible. An additional ~3 to 7% was destroyed during the SME in both runs. Nitrate difference was within analytical error for the SRAT cycles, but ~16% of the available nitrate in both runs was destroyed during the SME cycle.
- The peak CO<sub>2</sub> concentration was seen during the SRAT Decant 9 run (SB3A-9) and was ~30 volume percent. Significant peaks of CO<sub>2</sub> continued to be generated through the SME cycles. A carbon balance of the slurry system showed that a small percentage of the input carbon was not accounted for in the output carbon. More deviation was seen in the Decant 5 run (SB3A-8).
- The Decant 5 run had a peak nitrous oxide concentration of ~2.9 volume percent during the SRAT, while the Decant 9 run had a peak nitrous oxide of ~0.75 volume percent. Nitrous oxide continued to be generated throughout the SME cycles, but at much lower percentages.
- Rheological analyses of the SRAT and SME products were completed, and a report will be written by the ITS Rheology team evaluating the impacts on DWPF processing once the additional work on a simulant that more closely matches the anticipated SB3 composition is completed. Preliminary rheology data indicated that the SRAT product from the Decant 5 run (SB3A-8) was Newtonian in nature, while the SRAT product from the Decant 9 run (SB3A-9) exhibited non-Newtonian behavior. This was consistent with the preliminary results from the Phase I studies with the Decant 5 and Decant 9 SRAT products. The SME products from each run also exhibited different behaviors; however, it appears that settling may have affected the results. SME product rheological characterization will be further evaluated as part of the additional SB3 studies once the composition is finalized. The effect of processing temperature on rheology was not studied as part of either phase of the testing. The temperature effect will be studied on the simulant that more closely matches the anticipated SB3 and sludge batch 2 (SB2) combination.

Tank 7 sample analyses have indicated that low concentrations of oxalate will be present in SB3, which will impact the washing scenarios and final composition. Current plans are also considering co-processing of sludge SB2 with SB3. Once the projected washing scenario is defined, the sludge slurry composition will be evaluated against the existing SB3 chemical process cell processing window. Additional runs may be performed to help refine processing conditions. Bounding acid addition amounts will also be considered as part of those runs. This evaluation will be necessary to recommend a processing strategy for the Shielded Cells runs with the SB3 qualification sample.

## 2.0 INTRODUCTION AND BACKGROUND

The Phase I SB3 Simulant flowsheet runs were performed in November 2002 to evaluate four possible decant scenarios. The flowsheet runs are required for each sludge batch that is processed in DWPF so an evaluation of potential chemical processing issues, quantification of the potential hydrogen generation rates, and estimation of the required acid stoichiometry for that sludge batch can be made. Historically, DWPF has modified its operating flowsheet as necessary to adjust for processing of the incoming or existing sludge batch.

SRTC was requested by DWPF via Technical Task Request (TTR) HLW/DWPF/TTR-02-0016 to perform flowsheet studies to qualify SB3.[2] In response to this TTR, a Task Technical & Quality Assurance Plan [3] was written outlining the activities and controls necessary to meet the objectives and requirements of the TTR. The task plan outlined a two-phased approach to meet the objectives. The first phase, Phase I, performed tests to assist in the determination of the acid addition equation and to bound the possible processing scenarios for sodium oxalate in SB3 processing. The results of the Phase I testing were documented in WSRC-TR-2003-00088.[1] The second phase, Phase II, commenced once the final form of the acid addition and redox equations were determined with the focus to bound the SB3 processing window for acid addition. Since the time of planning the Phase II testing, both equations, along with their associated data, have been technically reviewed and finalized.[4,5] For the redox equation, slight adjustments to the coefficients were made.[5] Originally, the Phase II run objectives also included an attempt to define the processing strategy for the Shielded Cells run with the qualification sample (Shielded Cells run will be performed as a separate TTR). However, this may not be possible due to the dramatic difference seen in the actual Tank 7 analyses. Due to this change, the Phase II runs were halted after the completion of the excess acid runs. Slurry Mix Evaporator

(SME) cycles were not performed in Phase I, but were performed as part of Phase II using Frit 202 at a 35wt% waste oxide loading. Frit 202 does not necessarily represent the optimum frit for the projected SB3 composition, but was readily available and did have a processing window.

SB3, the next sludge batch to be qualified for DWPF, will consist primarily of Tank 7 sludge and the heel remaining in Tank 51. Based on projected compositions and the initial Tank 7 results, SB3 is expected to contain higher levels of noble metals than previously processed sludge batches.[6,7] Several components that are considered non-typical to DWPF sludge were also projected to be present. The non-typical components include: an H-Canyon slurry containing precipitated Pu with Gd; an Am/Cm stream; sand and coal from a sand filter that was discarded in Tank 7; and an appreciable amount of sodium oxalate. Material from Tank 18, which contains material (including zeolite) from Tank 19, will also be part of SB3. A stream of sludge with monosodium titanate (MST) from the Actinide Removal Process (ARP) will most likely be fed to DWPF during SB3 processing. The flowsheet studies addressed the inclusion of the sand, coal, and sodium oxalate in Tank 7, the Tanks 18 and 19 materials (from a composition perspective versus the actual zeolite material present in Tank 19), and the H-Canyon slurry stream. The studies did not attempt to bound the addition of the Am/Cm stream; however, limited testing with the feed has been performed by the Waste Processing Technology Section, along with a literature review and paper study.[6] The stream of MST from the ARP was also not completely addressed. Impacts of the addition of the oxalate portion of the stream (which would appear to have the largest impact on processing in the chemical process cell) have been bounded by the testing performed.

Sodium oxalate was projected to be present in Tank 7 at levels up to 660,000 pounds.[8] However, not all of this material would be processed in DWPF because some amount of washing and decanting of the Tank 7 sludge would be necessary to ensure that the material could be transferred and processed. SRTC used predictions by H.H. Elder of High Level Waste – Program Development and Integration to bound the sodium oxalate levels for processing. Throughout the SRTC SB3 studies, Elder's Decants 5 and 9 have been used as the baseline operating cases to set the sodium oxalate levels. Decant 5 corresponds to approximately 69% remaining sodium oxalate in Tank 7, while Decant 9 corresponds to approximately 40% remaining sodium oxalate<sup>1</sup>. Both of these compositions were tested at what was considered nominal acid levels at the time during Phase I. The Phase I runs, however, used only 10% of the projected levels of noble metals to bound nitrite destruction for the decant scenarios.

In addition to the objective of determining minimum acid addition required for the four decant scenarios, the Phase I tasks also provided the following information:

- Hydrogen, carbon dioxide, and nitrous oxide generation rates from processing SB3 simulant sludge at varying supernate anion concentrations and low levels of noble metals;
- The amount of oxalate remaining after the SRAT cycle at varying supernate anion concentrations; and
- The processing impacts (i.e., rheology and hydrogen generation) of sand, coal, and oxalate.

Changes to the DWPF acid addition strategy have been proposed based on the results of the SB3 chemical process cell scoping and Phase I studies. After the completion of the Phase I studies, a new acid addition equation was derived that was used for the Phase II runs. The methods utilized to derive the new acid addition equation were documented in WSRC-TR-2003-00118.[4] Based on input data from the equation and the results from the earlier SB3 scoping runs, estimates on the upper limit for acid addition were also made. This estimate included an upper bounding interval on the acid addition demand per liter of sludge slurry and was based on the prediction of the acid addition demand versus the actual acid used in Run SB3-21.[9,10] Run SB3-21 was selected since it exceeded the DWPF SRAT hydrogen limit and was also performed with a SME cycle. The upper bound for a particular feed was then based on the interval between its predicted acid demand and the limit imposed by Run SB3-21; resulting in a different upper bound for each feed. Testing the upper bounds was the main objective of the Phase II SB3 flowsheet studies. This was part of the TTR request, but the intent was also to provide DWPF with an upper acid addition level that could be used to adjust slurry rheology as necessary. The Phase II runs contained the nominal level of noble metals since their concentration directly impacts the amount of hydrogen generated.

No problems with nitrite destruction were anticipated, because the acid levels used in Phase II were upper bounds. The runs, however, were intended to provide the following information when excess acid was added:

- Affect on redox control (amounts of anions remaining after the SRAT and SME cycles);
- Hydrogen, carbon dioxide, and nitrous oxide generation rates from processing SB3 simulant sludge at varying supernate anion concentrations; and

---

<sup>1</sup> Decant values are per e-mail from H.H. Elder dated 7/30/02.

- Processing impacts (i.e., rheology and hydrogen generation). Any unusual observations during processing were also noted and will be reported.

A total of six runs have been performed as part of the Phase I and Phase II simulant flowsheet testing, and they were identified as follows:

Phase I	SB3A-1	SB3 Decant 5 composition, nominally 69% remaining sodium oxalate, 100% acid <sup>2</sup>
	SB3A-2	SB3 Decant 9 composition, nominally 40% remaining sodium oxalate, 110% acid
	SB3A-3	SB3 Decant 7 composition, nominally 52% remaining sodium oxalate, 110% acid
	SB3A-4	SB3 Extremely washed sludge, ~1% remaining sodium oxalate, 111% acid
Phase II	SB3A-8	SB3 Decant 5 composition, nominally 69% remaining sodium oxalate, 125% acid
	SB3A-9	SB3 Decant 9 composition, nominally 40% remaining sodium oxalate, 135% acid

This report will primarily focus on the results from Phase II, Runs SB3A-8 and SB3A-9.

### 3.0 EXPERIMENTAL

The experimental section is divided into three subsections. The first, Section 3.1, describes the sludge simulant used in the Phase II testing. Section 3.2 describes the procedures and equipment utilized in the testing. Finally, Section 3.3 discusses the acid addition strategy.

#### 3.1 Sludge Simulant and Slurry Preparation

The runs were performed using the same SB3 simulant used in the Phase I testing which was prepared at the Clemson Environmental Technologies Laboratory (CETL). The sludge is representative of the primary or traditional sludge components. The composition of the as-fabricated SB3 surrogate (without supernate adjustment) and the projected SB3 composition [6] are given in Table 1. The SB3 surrogate as fabricated is low in Na. This was done intentionally to allow for adjustments for the washing/decants and to allow for addition of the different levels of sodium oxalate. All of the other components in the SB3 simulant are slightly higher than the projected SB3 composition, but should match the projected composition once the sludge is trimmed with additional sodium oxalate or other species to match the predicted anion concentrations from Elder.

Large batches of the Decants 5 and 9 sludges were prepared for the flowsheet testing. A portion of these same simulants were used in the Phase I testing. The decant sludges, however, did not contain the non-typical or small sludge contributing components. Therefore, trim chemicals were added to the decant simulants to represent the sand, coal, gadolinium, mercury, and noble metals present in SB3. On a sodium oxalate free - dried sludge solids basis, the addition levels were 0.076 wt% mercury, 1.12 wt% sand (nominal range of 0.4 to 0.5 mm), and 0.72 wt% coal (nominal range of 0.6 to 0.8 mm).<sup>3</sup> The projected levels of noble metals are shown in Table 2 and are based on the La-139 content of SB3 [6]. As stated earlier, Phase I used only 10% of the target levels shown in Table 2. The actual amounts of the added trim chemicals are noted in Table A-1 of Appendix A. While the actual percentages added changed slightly from run to run; the ratio to Fe (a major sludge component) was maintained throughout the testing. The sand and coal are from the vendor of the sand filter material that was believed to have been transferred to Tank 7.

<sup>2</sup> At the time of testing and with the equation being used during Phase I, acid was 100%. Based on the new equation documented in WSRC-TR-2003-00118 and subsequent testing, the acid stoichiometry was determined to be 95%.

<sup>3</sup> Values for sand and coal are per e-mail from H.H. Elder dated January 25, 2002. These values are based on numbers reported by J.R. Fowler in DPST-80-409 and R.E. Eibling and J.R. Fowler in DPST-83-313. Value for mercury is from DPST-84-556 by J.R. Fowler.

**Table 1 – Sludge Compositions (Wt% Calcined Basis)**

Element	SB3 Simulant Composition*	Projected SB3 Composition**
Al	13.0	11.02
Ba	0.276	0.26
Ca	3.35	2.96
Ce	N/A	0.34
Cr	N/A	0.29
Cu	0.211	0.18
Fe	38.3	32.4
K	0.273	0.41
La	N/A	0.20
Mg	0.258	0.13
Mn	7.48	6.40
Na	1.32	9.08
Ni	1.33	1.45
Pb	N/A	0.32
Si	1.15	1.13
Zn	0.429	0.38
Zr	0.225	0.66

\*Simulant composition represents an average of analyses performed on duplicate samples by the SRTC-Mobile Lab on 9/24/02.

\*\*Per Reference 6.

N/A – Element was not added to the SB3 simulant

**Table 2 - Projected Levels of Noble Metals (Sodium Oxalate Free - Dried Solids Basis)**

Species	10% Addition Amount	Nominal Amount*
Ag	5.42 E-05 wt%	5.42 E-04 wt%
Pd	2.76 E-03 wt%	2.76 E-02 wt%
Rh	5.11 E-03 wt%	5.11 E-02 wt%
Ru	1.83 E-02 wt%	1.83 E-01 wt%

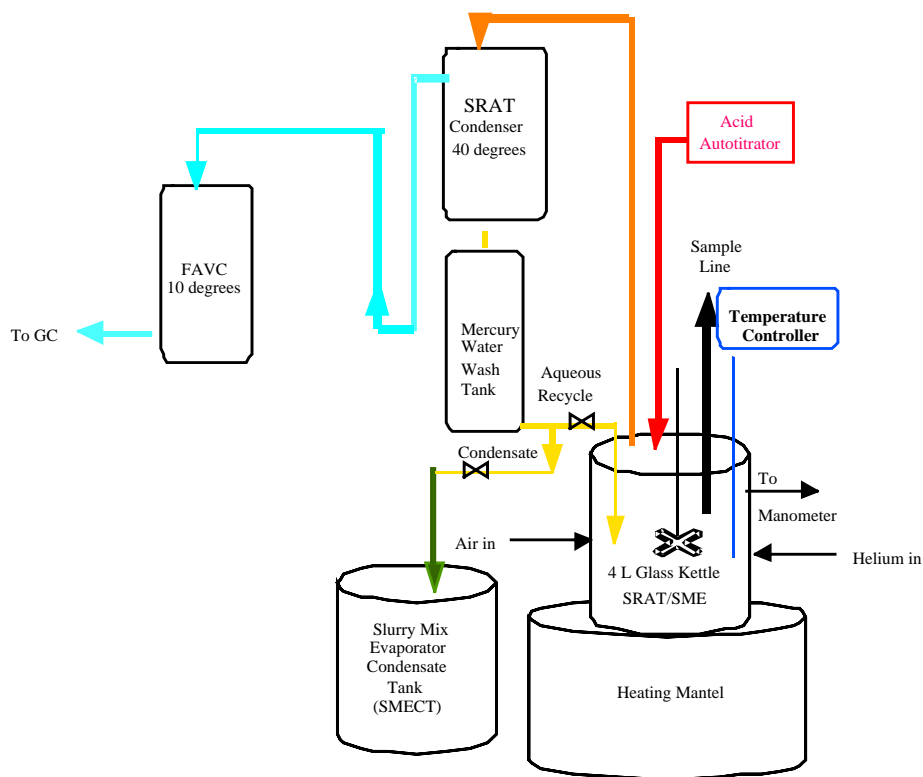
\*Per Reference 4

### 3.2 Procedures and Equipment Used in Testing

The testing was once again performed at the Aiken County Technology Laboratory (ACTL) using a four-liter kettle with various glassware fabricated to functionally replicate the DWPF processing vessels. A 4-liter glass kettle is used to replicate both the SRAT and the SME, and it is connected to the SRAT Condenser, the Mercury Water Wash Tank (MWWT), the Slurry Mix Evaporator Condensate Tank (SMECT), and the Formic Acid Vent Condenser (FAVC). For the purposes of this paper, the condensers and wash tank are referred to as the offgas components. A sketch of the experimental setup is given as Figure 1.

SRAT/SME processing followed the run plans written for each run.[11,12] The runs were performed in accordance with Procedure 2.02 (“Laboratory Scale Chemical Process Cell Simulations”) of Manual L27 [13]. Slurry pH and offgas hydrogen, nitrous oxides, and carbon dioxide concentrations were measured during the experiments using in-line instrumentation, so that total amounts generated and peak generation rates could be calculated. Slurry samples were pulled during processing to monitor the oxalate, nitrite, nitrate, and formate concentrations in the slurry. During the runs, the kettle was monitored to observe reactions that were occurring during each run to include foaming, air entrainment, rheology changes, loss of heat transfer capabilities, and offgas carryover. Observations were recorded in laboratory notebook WSRC-NB-2002-00194 and are discussed in Section 5.

Figure 1 – Schematic of SRAT Equipment Set-Up



Concentrated nitric acid (50-wt%) and formic acid (90-wt%) were used during processing. In addition, 200 ppm IIT 747 antifoam was added during heat-up at 40°C, and an additional 400 ppm was added at the completion of acid addition. The addition strategy was conservative relative to the current DWPF addition strategy to increase sensitivity to foaming issues, and no recommendations on changes to the antifoam addition strategy will be made until the completion of qualification runs. SRAT processing included the dewater time in boiling plus an additional 12 hours of reflux to simulate DWPF processing conditions. As part of the SME cycle, the equivalent of five decontamination canister additions were replicated. Each addition was followed by a return to boiling and dewatering. Three frit additions were performed as part of the SME cycle with subsequent concentrations after each addition.

Samples of the SRAT and SME slurries and products were characterized for chemical composition and physical properties. Samples from the SMECT, FAVC, and MWWT were also characterized. Rheology samples of the SRAT and SME product were also taken for rheology characterization.

### 3.3 Acid Addition Strategy

As stated earlier, a major focus of the Phase I SRAT runs was to assist in refinement of the acid addition equations for SB3. An acid addition equation was developed [4] and is given as equation 1.

$$\text{Eq (1) moles acid} = V_s * \left[ 1.47 * [\text{B.E.}] + \rho_s * \left( \frac{1.95 * [\text{NO}_2^-]}{46.007} + \frac{[\text{Hg}]}{200.6} + \frac{0.55 * [\text{C}_2\text{O}_4^-]}{88.02} \right) \right] * \text{factor}$$

where:  $V_s$  is the SRAT receipt slurry volume, L  
 $\rho_s$  is the SRAT receipt slurry density, kg/L  
 [B.E.] is the SRAT receipt base equivalents at pH 7, equivalent moles OH-/L  
 [NO<sub>2</sub><sup>-</sup>] is the SRAT receipt mass of nitrite ion per unit mass slurry  
 [Hg] is the SRAT receipt mass of mercury per unit mass slurry  
 [C<sub>2</sub>O<sub>4</sub><sup>-</sup>] is the SRAT receipt mass of oxalate per unit mass slurry  
*factor* is a multiplier to increase the total acid above that predicted by the four terms

This equation gave the total acid necessary to achieve neutralization of the measured hydroxides and carbonates, destruction of nitrite, reduction of a fraction of the Mn<sup>4+</sup>, reduction of Hg, and adjustment of the melter feed rheology to DWPF operating conditions. Since the objective of the Phase II runs was to define the upper bound for acid addition, higher quantities than stoichiometric acid addition were used. A preliminary estimate of the upper bound was made using the results from the earlier SB3 scoping studies and the Phase I studies. An earlier SB3 scoping study run at 75% remaining sodium oxalate and the nominal noble metals (Run SB3-21) did exceed the DWPF SRAT hydrogen limit.[9,10] This addition amount was assessed against the new acid addition equation (Eq 1) and the excess acid margin was used to estimate the equivalent amount of acid for the Decant 5 and 9 runs. This amount turned out to be ~25% more acid for each run.

An interim redox algorithm developed by Jantzen was then used to determine the acid mix to produce the redox target. Although a Fe<sup>2+</sup>/ΣFe of 0.200 was targeted, an error in the input formula actually resulted in the target being 0.226. This was discovered after the completion of the testing when the redox prediction was being made for the as produced material. Equation (2) was the interim SB3 redox equation utilized in this testing. Equation (2) is slightly different than the final recommended equation for SB3, with an intercept of 0.179 instead of 0.175 and a slope of 0.196 instead of 0.235.[5]

$$\text{Eq (2)} \quad \frac{Fe^{+2}}{\Sigma Fe} = 0.175 + 0.235 * (2 * \text{Formate} + 4 * \text{Oxalate} + 4 * \text{Coal} - 5 * (\text{Nitrate} + \text{Nitrite}) - 2 * \text{Mn})$$

where the input values are in the units of gram-moles of species per kilogram of melter feed slurry.

Based on earlier SB3 studies [4,9], some assumptions on the SRAT/SME reactions and anion destruction were made to calculate the total acid and the split between nitric and formic acid. They were:

- 100% nitrite destruction;
- 0% nitrite to nitrate conversion ; and
- 30% total formate destruction and 20% total oxalate destruction.

Run SB3A-8 used 125% of the calculated stoichiometric addition with ~65% of the moles of acid provided by formic, Run SB3A-9 used 135% of the calculated stoichiometry with ~70% of the moles of acid provided by formic.

#### 4.0 ANALYTICAL

A high-speed micro Gas Chromatograph (GC) was used during the experiments to monitor the generated gases for hydrogen, oxygen, nitrogen, carbon dioxide, and nitrous oxide. Monitoring these species provides insight into the reactions occurring during processing and demonstrates whether a flammable mixture is formed. Helium was used as a GC internal standard and was also monitored during the runs. The GC is self-contained and is designed specifically for fast and accurate analysis. The GCs had five main components. The first is the carrier gas (argon for this testing) to transport the sample through the molecular sieve and poraplot Q columns. The second is the injector, which introduces a measured amount of sample into the inlet of the analytical columns. The amount of sample injected depends on the length of time the injector is open. The injected sample flows to the analytical column where it is separated. The third component is the column, which is the separation system. The column is capillary tubing coated or packed with a chemical substance known as the stationary phase that preferentially attracts the sample components. As a result,

components separate as they pass through the column based on their solubility. Since solubility is affected by temperature, column temperature is controlled during the run. The fourth component is a micro-machine thermoconductivity detector. The solid state detector monitors the carrier and senses a change in its composition when a component in the sample elutes from the column. The fifth component is the data system, EZChrom. Its main purpose is to generate both qualitative and quantitative data. It provides a visual recording of the detector output and an area count of the detector response. The detector response is used to identify the sample composition and measure the amount of each component by comparing the area counts of the sample to the analysis of known calibration standards. Two calibration standards were used and consisted of 0.5% and 0.8% helium, 1.0% hydrogen, 12.0% and 20.0% oxygen, 10.0% and 25.0% carbon dioxide, and 1.0% and 15.0% nitrous oxide. The calibration standard is balanced in argon because helium was used as an internal standard and was used to detect leakage during the actual run.

Analyses for this task used guidance of Analytical Study Plan (ASP) WSRC-RP-2002-00577.[14] Sample request forms were used for samples to be analyzed, and analyses followed the guidelines and means of sample control stated in the ASP for the task. A unique lab identification number was assigned to each sample for tracking purposes. Analyses were performed using approved analytical and QA procedures.

Samples were taken before the runs were initiated, throughout the runs, and at the end of the runs for analyses to quantify the processing behavior. The samples were analyzed by the Immobilization Technology Section - Mobile Lab (Mobile Lab), the Immobilization Technology Section (ITS), and the Analytical Development Section (ADS). The Mobile Lab analyzed the initial and product samples to determine the soluble and insoluble species. Initial sludge, SRAT product, and SME product samples were prepared in duplicate for cation chemical analyses by calcining a portion of the samples at 1100°C and then dissolving the calcined product using Na<sub>2</sub>O<sub>2</sub>/NaOH fusion, lithium metaborate fusion, and aqua regia dissolution. Cation analyses were performed using Inductively Coupled Plasma – Atomic Emission Spectroscopy (ICP-AES). Anion analyses were performed using weighted dilutions and Ion Chromatography (IC). Samples analyzed for oxalate had to undergo an additional preparation step before analyses, and they were prepped using a HCl/HNO<sub>3</sub> strike. To obtain the composition of the soluble fraction of the samples, the SRAT and SME products were prepped by filtering the slurry samples to remove the supernate. The resulting filtered supernate was then analyzed using ICP-AES and IC. The initial sludge samples, SRAT products, and SME products were also analyzed for solids content. The total and dissolved solids were measured on two aliquots and the insoluble and soluble solids fractions were calculated from the results. ITS performed the titration on the starting sludges in duplicate to provide the necessary input for the acid calculation. Lastly, the ADS measured the total inorganic carbon/total carbon of the decant sludges and the SME products.

The Mobile Lab analyzed the in-process samples to determine the anions present. This data was used to help determine the reactions that occur during SRAT and SME processing, including the destruction rate of the nitrite. In-process samples for anion analyses were diluted with a 1 N NaOH solution immediately after the sample was removed from the vessel during the run. A weighted dilution was performed on these samples, and they were then analyzed using IC. The additional HCl/HNO<sub>3</sub> strike had to again be performed to measure the oxalate concentration. An in-process supernate sample was also taken at the end of acid addition. This sample was centrifuged and the resulting supernate was decanted and analyzed.

Due to the large amount of material condensed during the runs and the darker appearance of the condensate compared to other runs, samples from the FAVC, the MWWT, and the SMECT (from SRAT dewater only) were also submitted to the Mobile Lab for analyses. The solutions were analyzed using ICP-AES and IC. The archived samples from Phase I were also analyzed for comparison. The results will be reported and discussed in Section 5.3.

The rheological properties of the SRAT and SME products were measured by the ITS. A 125-ml SRAT and SME product sample was pulled for rheological characterization from each of the runs. The samples were run at the existing total solids. The sample jacket temperature was 25°C and the Z41 geometry was used to perform the analyses. Due to the anticipated changes to the SB3 composition that will actually be processed in DWPF, additional rheological characterization will be performed once the new SB3 sludge slurries matching the Tank 51 composition are fabricated. The effect of temperature will also be measured for these samples. Upon completion, a rheology report will be written to include the testing done with the Phase I and Phase II samples. Preliminary results are reported in Section 5.3.

## 5.0 SRAT/SME RUN RESULTS

The data from the testing and any observations will be discussed in the next two sections. This section has been divided into three subsections. Section 5.1 will discuss the analyses of the starting sludges and the necessary inputs for the acid calculation. Section 5.2 will discuss the results of the in-process samples, generated gas data, and general observations about processing. Finally, section 5.3 will discuss the product analyses. Section 6.0 provides the system mass balances.

### 5.1 Starting Sludge Composition

As mentioned above, the SB3 simulant was the same as that used in the Phase I testing. Before the runs were initiated, a sample of the starting sludges was removed for chemical analyses. The composition of the untrimmed sludge was given in Table 1. The target and measured sludge compositions trimmed to match the decant compositions are given in Table 3, but do not include the contribution from Gd, Hg, noble metals, sand, and coal. Chemical analysis methods were described in Section 4.0.

The analyses of the cations in the initial sludges indicate that the target compositions were fairly well met. The only major sludge component that was  $\geq \pm 10\%$  from the target was Na in the SB3A-8 sludge, which could be the result of a non-representative sample of the sodium oxalate present. The target Na for the SB3A-9 sludge was within 10%. The minor sludge components, Ni and Si, also were not within  $\pm 10\%$  of the target, but, since these are minor components, this did not present a problem for processing.

**Table 3 – Initial Sludge Composition: Target and Measured Comparison (Dried Solids Basis)**

Element	SB3A-8		SB3A-9	
	Target <sup>1</sup>	Measured <sup>2</sup>	Target <sup>1</sup>	Measured <sup>2</sup>
Al	5.35	5.05	7.14	6.69
Ba	0.12	0.126	0.16	0.165
Ca	1.43	1.55	1.91	2.03
Cu	0.09	0.078	0.12	0.106
Fe	15.59	14.3	20.80	18.9
K	0.15	0.233	0.20	0.353
Mg	0.13	0.107	0.17	0.145
Mn	2.90	3.00	3.87	3.92
Na	18.03	16.1	12.30	11.1
Ni	0.65	0.558	0.87	0.782
Si	0.56	0.654	0.75	0.811
Zn	0.18	0.180	0.24	0.238
Zr	0.31	0.292	0.42	0.384

<sup>1</sup>Based on decant compositions provided by Elder that were subsequently adjusted to remove the uranium component.

<sup>2</sup>Chemical analysis was performed on two aliquots removed from the submitted sample. Results represent an average of the duplicate analyses. P and Gd are not reported since they were below the detection limit.

The starting sludge was also analyzed for the anion components using a weighted dilution method and IC. The Mobile Lab results are given in Table 4. Table 4 also shows the targeted concentrations. A comparison of the data indicates that the target anion concentrations were fairly well met for SB3A-8. The SB3A-9 sludge, on the other hand, was ~23% high in nitrate and ~23% low in oxalate. The decision was made to use the feed as is and the revised input values were used to calculate acid demand. The lower oxalate results in both cases help support the slightly low Na reported in Table 3, providing further indication of low representation of the sodium oxalate in the initial sludge sample. However, for Run SB3A-8, the difference in the measured versus target Na can not be completely attributed to the low oxalate concentration.

**Table 4 – Initial Sludge Slurry Anion Concentrations (mg/kg slurry)**

Anion	SB3A-8		SB3A-9	
	Target <sup>1</sup>	Measured <sup>2</sup>	Target <sup>1</sup>	Measured <sup>2</sup>
Nitrite	8,404	8,750	2,325	2,470
Nitrate	2,413	2,580	1,330	1,630
Oxalate	41,750	39,700	29,480	22,750

<sup>1</sup>Target is based on decant scenarios and known addition amounts of trim chemicals.

<sup>2</sup>Measurement represents results of duplicate analysis except for oxalate for SB3A-8.

The total and dissolved solids were measured on duplicate samples of the starting sludges. These results were then used to calculate the insoluble and soluble solids content of the starting sludge. The results are presented in Table 5. As discussed earlier, calcination of the sludge is performed to prepare the sludge for chemical analyses; the calculated calcined solids from this preparation are given in Table 5. An initial slurry density and pH were also measured and the data are given to complete the physical property characterization of the starting sludge.

**Table 5 - Physical Properties of the Initial Sludge**

Run ID	Total Solids <sup>1</sup>	Insoluble Solids <sup>2</sup>	Soluble Solids <sup>2</sup>	Calcined Solids <sup>1</sup>	Slurry Density (g/ml)	pH
SB3A-8	17.6%	13.0%	4.60%	11.8%	1.14	12.1
SB3A-9	18.5%	14.5%	3.97%	13.1%	1.14	12.2

<sup>1</sup>Performed on duplicate aliquots from initial sludge sample. Data represents average of the two measurements.

<sup>2</sup>Insoluble and soluble solids are calculated from the measurement of total and dissolved solids.

The target total solids was 18% for SB3A-8 and 18.8% for SB3A-9, so the initial sludges were fairly close to the target. The lower insoluble solids and higher soluble solids for SB3A-8 are consistent with previous SB3 results seen with higher oxalate levels.[10] The target calcined solids for SB3A-8 was 12%, while it was 13.3% for SB3A-9. Both were close to the target. SB3A-9 sludge had the greater amount of calcined solids and the higher ratio of calcined to total solids. The target slurry density was 1.13 g/ml so both sludges were close to the target. Little variation was seen in the measured slurry densities and the sludge pH.

Since the current DWPF acid addition equation requires input for the amount of total inorganic carbon (TIC), the carbon content of the starting decant sludges was also measured by ADS. The slurry samples were ground to try to ensure homogenization of the sample before introduction into the analyzer. The total carbon (TC), total inorganic carbon (TIC), and total organic carbon (TOC) results are given in Table 6. The inorganic carbon reported values were slightly more than anticipated. The result for total carbon for Run SB3A-8 was a little lower than anticipated; whereas, the value for Run SB3A-9 was greater than anticipated. Some of the deviation could be attributed to difficulty in obtaining a representative sample of the oxalate in the sludge. The exact explanation for the differences has not been determined; however, variations in the measured inorganic and total carbon have been seen in the scoping SB3 and the Phase I studies.[1,10] The errors are believed to be attributed to the presence of oxalate, and preliminary Tank 7 results suggest that oxalate will not be present in SB3 at the levels tested. Therefore, this should not be a concern. Also, the proposed SB3 acid addition equation also does not rely upon TIC as an input, so the effect of the error is minimized.[4] Errors in the total carbon values are less problematic since they are used as a verification of other inputs.

**Table 6 – Carbon Analyses on Starting Sludge (µg/ml)**

Run ID	Total Carbon <sup>1</sup>	Inorganic Carbon <sup>1</sup>	Organic Carbon <sup>2</sup>
SB3A-8	13,100	1,210	11,890
SB3A-9	8,980	1,150	7,830

<sup>1</sup>Performed on single sample that was ground to ensure homogeneity.

<sup>2</sup>Organic carbon is calculated by difference from total carbon and inorganic carbon measurement.

The starting sludge for each run was titrated by ITS using an autotitrator and a 30:1 dilution of the starting slurry. This is similar to the method used by the DWPF. The results are given in Table A-1 of Appendix A and were in-line with results seen in the Phase I runs with the same decant composition.[1]

## 5.2 SRAT and SME Processing

As stated in Section 3.2, the two SRAT runs were performed simultaneously in two different hoods at the ACTL in the 4-liter vessels. The individual sludges and trim chemicals were added to the vessels prior to the start of the SRAT tests. The runs were started by heating up the vessels. Several operating problems occurred with the Temp-O-Trol temperature control box in Run SB3A-9 causing it to be changed out twice. This resulted in an increased time for acid addition by approximately 1 hour, but the acid addition rate was maintained during the addition to be consistent with the DWPF acid addition rate. Antifoam was added at 200 ppm when the slurry reached ~40°C. Acid addition was started when the slurry reached 93°C. Nitric acid was added first and then formic acid. During nitric acid addition for Run SB3A-8, problems with the measured He concentration were experienced. Acid addition was stopped and the vessel was cooled so a leak check could be performed. The leak check was satisfactory, so additional investigation to identify the problem was performed. The GC and the flow meters were changed to ensure that they were not the cause of the problem. Finally, after ~8 hours of investigation, an acceptable He flow rate was obtained. Heating was then resumed and nitric acid addition began after the slurry reached 93°C. After the completion of formic acid addition, 400 ppm of antifoam was added and then the vessel was ramped to boiling. Once boiling was initiated, the SRAT contents were dewatered/concentrated to bring the sludge to the starting solids concentration. Just as the dewatering was being completed for SB3A-9, the air flow disappeared. It was determined that the shared air cylinder had emptied due to its dual use with other ACTL equipment. The air flow was absent for ~15 minutes, but it occurred during the peak hydrogen generation. Therefore, the air flow was increased for a brief period (~5 minutes) to flush the hydrogen that had accumulated in the SRAT vessel. This delayed the sampling of the slurry sample to be taken at the end of the SB3A-9 dewater also. After dewatering was complete, the goal was to reflux the SRAT for 12 hours. This was done for Run SB3A-9 but due to all of the problems that occurred in Run SB3A-8, confusion over the start of boiling and the actual processing time required resulted in reflux only being performed for 10 ½ hours. The total boiling time for Run SB3A-8 was 12 hours.

The equivalent water amount from five canister decontaminations was added during each SME cycle. Each addition was 430 ml, which was added over 10 minutes at a rate of 43 ml/min. The vessel was re-heated to boiling after each addition then the added amount was dewatered. After the fifth canister addition dewater, the frit addition cycles were started. The frit was added over 3 additions with formic acid and water. The acid and water addition amounts were based on the DWPF target frit slurry addition method (i.e., 1.5 wt% formic in 50 wt% solid solution). After each frit addition, the SME was concentrated with a goal of reaching a final solids content of ~45 wt%. Processing parameters are given in Table A-1 of Appendix A. Mass balances of the components added and removed from the vessels are given as Table A-2 in Appendix A.

The pH was measured throughout the runs. No problems were experienced during Run SB3A-8. However, during nitric acid addition in Run SB3A-9, the pH measurement was not substantially changing. After formic acid addition started and no dramatic change in pH was seen, the pH probe was removed and a new probe was inserted. The formic acid addition was stopped for about 10 minutes to perform the change out. A check of the old probe in the pH 4 buffer indicated that the probe had failed. Therefore, the pH data for about 3 hours was considered invalid. Figure 2 is a plot of the measured pH during the runs and does not include the invalid data from Run SB3A-9.

The pH profiles were relatively similar. Run SB3A-8 reached a lower pH at the end of acid than Run SB3A-9 did. It also returned to a neutral pH much quicker than SB3A-9 did. Run SB3A-9 appeared to be consuming acid throughout refluxing, whereas SB3A-8 appeared to have completed consumption reactions ~6 hours into boiling based on the pH profile. Run SB3A-8 showed a dramatic change in pH during the second canister addition cycle with a slight drop in pH by the end of the frit cycle. The pH fluctuated between 7 and 8 throughout the SME cycle due to the addition of the decontamination canister water and the frit/water/formic additions. A more dramatic shift in pH was seen during frit addition. Both runs had roughly the same ending pH. Figure 3 shows a plot of the SRAT cycle pH for the Phase II runs compared to the Phase I runs with the same decant compositions and lower acid. The runs showed similar behavior during acid addition with the primary difference being the ending acid pH. In spite of the lower acid addition amounts used, the Phase I runs had a much lower pH after the completion of acid addition. This could be attributed to lower noble metals content. Scoping studies have shown this behavior in the past.[10,15] These results support the hypothesis that there is a consumption of acid catalyzed by the noble metals.

Figure 2 – pH Plots during SRAT/SME Processing

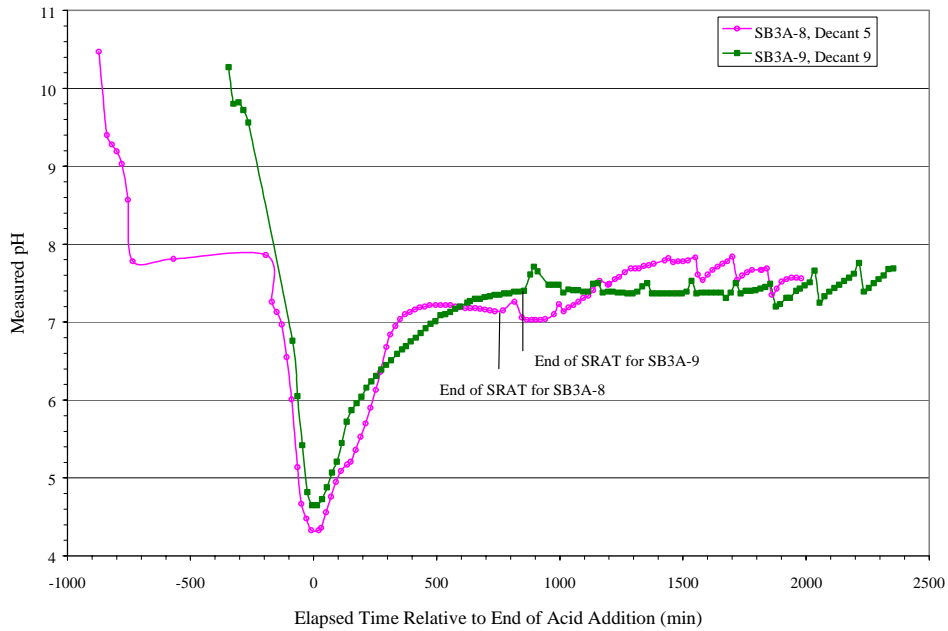
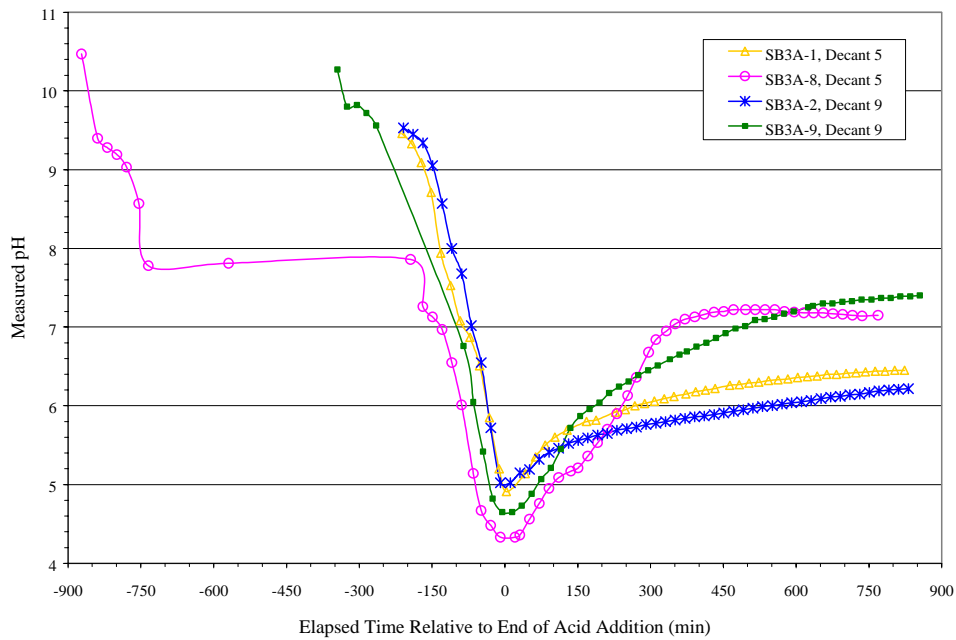


Figure 3 – pH Plots during SRAT Processing for Decants 5 and 9 in Phases I and II



Samples of the slurries were taken throughout processing to monitor the chemical reactions. Only one intermediate SME cycle sample was taken. The sample was taken at the end of the canister decontamination cycles and before the start of frit addition. The samples were quenched with NaOH and then submitted to the SRTC-ML for anion analyses. The sample results, along with the times the samples were removed relative to the end of formic acid addition, are given in Table 7. Two sets of data are provided for formate and oxalate. After questionable results from the first analyses, the samples were re-prepped and re-run for formate and oxalate. Dramatic differences in the oxalate data were seen. Based on the known amounts of oxalate in the starting sludge (see Table 4), it was determined that the first results for Run

SB3A-8 appeared to be more accurate, and the second set of results for Run SB3A-9 appeared to be more accurate. The formate results did not show a dramatic change and the results were averaged. The Mobile Lab attempted to find an obvious reason for this difference. However, none could be found. If the oxalate method is to be implemented in DWPF, more work on the method development may be necessary and the Mobile Lab will have to work with ADS to resolve some of the outstanding issues. In general, the impact of the changes to the data is minimal since they are mainly used to monitor relative destruction during the cycle. The values are used to calculate anion loss for the mass balances; however, they represent a small fraction of the anions present in the system. Therefore, slight variation in the concentrations should not greatly affect the calculated cycle destruction values.

The following system was used for the Sample IDs in the runs:

- the “-A” samples were taken at the end of nitric acid,
- the “-B” samples were taken 80 minutes into formic acid addition,
- the “-0” samples were taken at the end of formic acid addition,
- the “-1” samples were taken 30 minutes into dewatering,
- the “-2” samples were taken at the end of dewater, and
- the remaining samples were taken every 2 hours after the completion of dewater.

**Table 7– In-Process Slurry Anion Concentrations Based on Weighted Dilutions (mg/Kg)**

Run ID	Sample ID	Time Relative to End of Acid Addition (min)	Nitrite	Nitrate	Formate-Sample 1	Formate - Sample 2	Oxalate-Sample 1	Oxalate-Sample 2
SB3A-8	SRAT IC-A	-133	9080	30048	<109	<109	34620	28523
	SRAT IC-B	-49	7961	33205	26673	25257	37560	29830
	SRAT IC-0	1	600	31681	38539	37233	36689	28741
	SRAT IC-1	59	<108	33423	35818	38104	36471	30701
	SRAT IC-2	121	<108	37560	39628	37995	38539	29177
	SRAT IC-4	241	<109	36362	37560	35382	40499	34947
	SRAT IC-6	361	<109	36797	32987	28306	41261	33205
	SRAT IC-8	481	<108	35818	32007	30592	35600	26999
	SRAT IC-10	601	<108	37777	28632	24278	36144	29177
	SRAT IC-12	721	<109	36253	25911	26346	38213	30265
	SRAT IC-14	749	<109	36362	27761	23624	34947	26128
	SME IC-0	1548	<108	32443	19052	18943	37233	27217
SB3A-9	SRAT IC-A	-134	1319	21763	<107	<107	27873	19833
	SRAT IC-B	-35	1177	22037	26209	28883	29632	19255
	SRAT IC-0	3	486	22229	36867	39904	27434	20602
	SRAT IC-1	60	<109	23137	36780	37216	29686	21173
	SRAT IC-2	165	<109	25409	38386	39477	29226	22246
	SRAT IC-4	258	<108	24898	35138	38048	29964	23497
	SRAT IC-6	378	<108	24030	33988	37776	27385	24138
	SRAT IC-8	498	<108	24506	34438	35086	31416	25046
	SRAT IC-10	618	<108	22965	32390	31415	30873	24482
	SRAT IC-12	738	<108	21960	29857	32236	31263	22176
	SRAT IC-14	858	<109	23377	31132	27964	30914	22066
	SME IC-0	1868	<109	20544	24566	25110	36849	24892

Note: Performed on samples removed during processing that were quenched with 1 N NaOH. Data presents results from single analysis corrected for NaOH quench.

The nitrite data shows that the DWPF limit of <1000 mg/kg was met by the end of acid addition. This was much sooner than in the Phase I runs with lower acid and lower noble metals. In the Phase I runs, the Decant 5 run (SB3A-1) was met ~8 hours into reflux, while the Decant 9 run (SB3A-2) met the specification by the end of dewater/concentration. Nitrate ion concentration increased slightly during acid addition and then peaked at the end of dewater. The nitrate remained relatively steady throughout reflux and then decreased slightly by the end of the canister dewater cycles. The increase in nitrate concentration during acid addition may have been associated with conversion of nitrite. In general, formate concentration increased through dewater, then slowly decreased during the SRAT reflux and the SME cycle.

The trends were consistent between the two sets of data. Finally, oxalate concentration did not show a consistent pattern and varied from sample to sample. The reported concentration data indicates less oxalate present at the end of the SRAT cycle than at the end of the canister decontamination cycle (SME-IC-0). This could possibly have been attributed to analytical error with the analytical equipment or with the sample that was analyzed (i.e., difference in the amount of solids introduced in the sample analyzed) or may have been the result of oxalate reforming in the system after the SRAT was completed. This trend was also seen in the earlier SB3 scoping SRAT/SME runs.[10]

As mentioned in Section 4.0, hydrogen, oxygen, nitrogen, carbon dioxide, and nitrous oxide were measured throughout the runs using GCs. Figures 4 and 5 give the gas composition data measured by the GC for the runs. As mentioned above some problems with the helium concentration were experienced during Run SB3A-8. This resulted in the change out of the Channel A column of the GC and spurious readings at the start of run. During both runs, the air and helium flows had to be increased for a brief period due to excessive hydrogen generation. For Run SB3A-8, this was done for ~40 minutes, while for SB3A-9 it was the result of loss of airflow and was increased for ~5 minutes. Both runs used 1.5x the target air and helium purge rates. No other problems with the GCs were experienced during the runs. A slight break in the GC data is evident at the end of the SRAT run where the GCs were stopped and a calibration check was performed. Spikes in the measured concentrations are noted throughout the SME cycles and correspond to the times at which decontamination canister water or frit/water/formic was being added.

Figure 4 – GC Data from Run SB3A-8

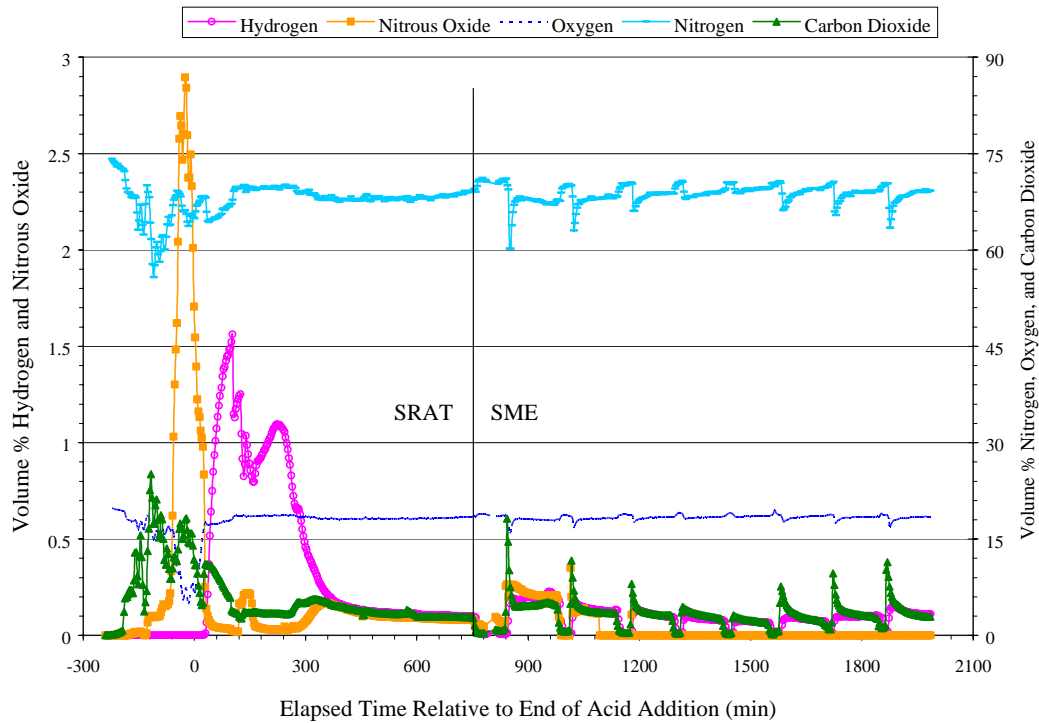
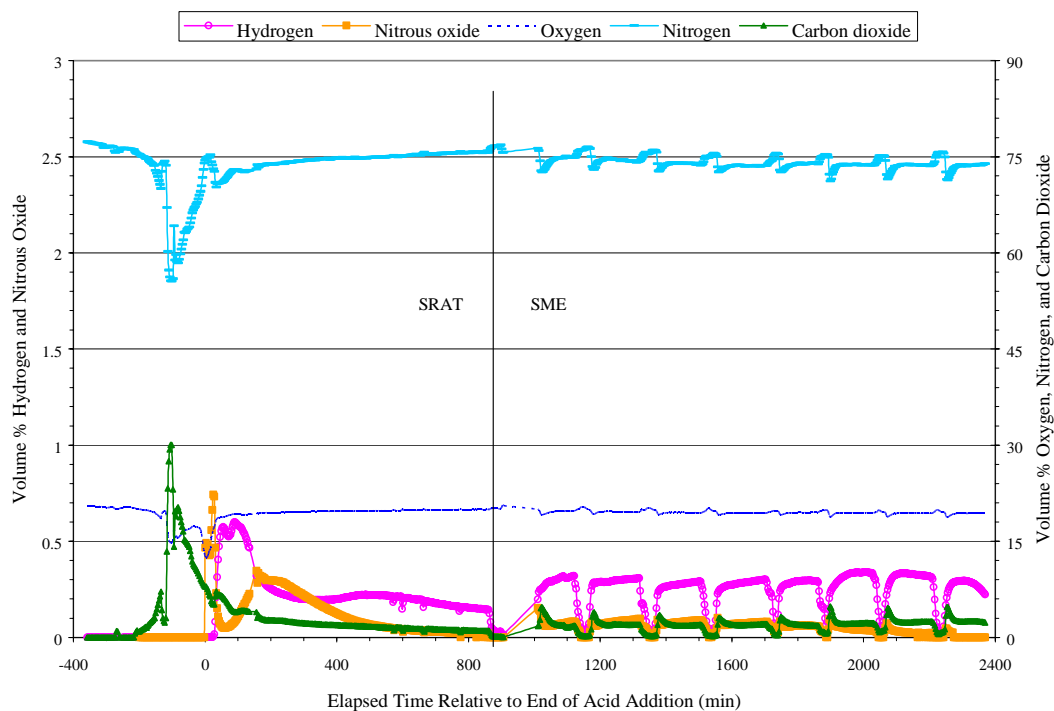


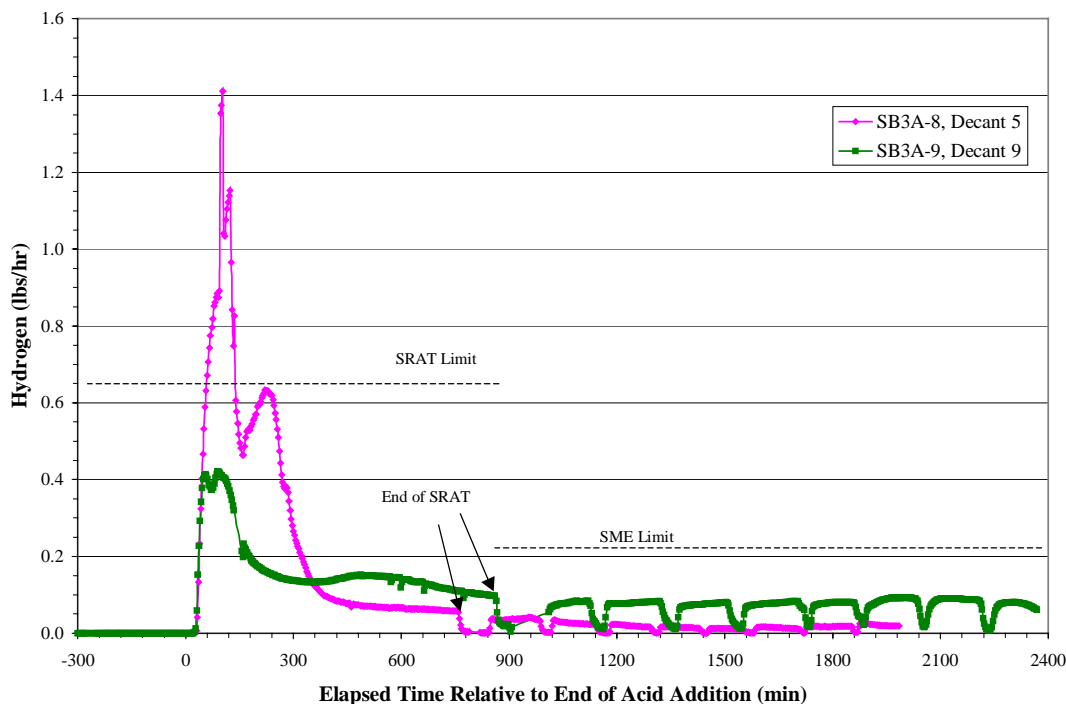
Figure 5 – GC Data from Run SB3A-9



Significant hydrogen was detected in both runs throughout the SRAT and SME cycles. To better evaluate the hydrogen generation, Figure 6 is provided and compares hydrogen generation for the two runs on a DWPF scale in pounds per hour. For Run SB3A-8, the SRAT peak occurred at ~103 minutes after the end of acid addition and was equivalent to 1.41 lbs/hr based on the DWPF scale (1/9165<sup>th</sup> of DWPF scale based on volume). In Run SB3A-9, the SRAT peak occurred at ~89 minutes after the end of acid addition and was equivalent to 0.421 lbs/hr on the DWPF scale (1/9165<sup>th</sup> of DWPF scale based on volume). The SME peak hydrogen generation was 0.038 lbs/hr for Run SB3A-8 and 0.093 lbs/hr for Run SB3A-9. SME hydrogen fluctuated with the canister decontamination and frit additions in the SME cycle, where hydrogen would drop as the material was added and the vessel cooled and then would increase again and plateau during dewater. The total hydrogen generated during the SRAT and SME cycles will be discussed in Section 6.0, along with an evaluation of the hydrogen data as it relates to the carbon dioxide generation.

Both runs exhibited similar behavior with respect to nitrous oxide generation. Peaks of nitrous oxide occurred at two distinct times during the SRAT cycle. The first occurred near the end of acid addition, which was just prior to the hydrogen peak. The second occurred around the time when the SRAT was switched from dewater to reflux. The presence of these two peaks was consistent with earlier SB3 simulant SRAT runs [10,15,16]. Peak nitrous oxide concentration was 2.9 volume percent for Run SB3A-8 during the SRAT and was 0.73 volume percent for Run SB3A-9 during the SRAT. Peak levels were lower during the SME cycle and were 0.35 and 0.15 volume percent respectively. During the SB3A-8 SME cycle, the nitrous oxide peaked with the first 3 canister decontamination additions then slowly tapered off during concentration. By the end of the third addition, no more nitrous oxide was generated. For the SB3A-9 SME, nitrous oxide continued to peak with every addition made to the SME. It finally went to zero by the end of the SME cycle. The nitrous oxide peaks for these high acid runs occurred sooner than in the nominal acid runs of Phase I.[1] Several peaks of carbon dioxide were seen in both SRAT cycles especially during acid addition. Other smaller peaks were generated when hydrogen or nitrous oxide started to peak. During the SME cycles, carbon dioxide dropped with each addition and then peaked once the vessel returned to boiling. Carbon dioxide remained elevated throughout the dewatering steps in the SME cycle. SRAT peak carbon dioxide concentration was 25 volume percent for SB3A-8 and 30 volume percent for SB3A-9, while the peak SME carbon dioxide concentration was 18 volume percent and 5 volume percent, respectively. The total nitrous oxide and carbon dioxide generated during the runs on a DWPF scale will be discussed in Section 6.0 where the system material balances are presented.

Figure 6 – Hydrogen Generation on a DWPF Scale



Based on the plots provided in Figures 4 through 6, the greatest amount of gases appeared to be generated during the SB3A-8 SRAT cycle, while the SME cycle for Run SB3A-9 had more generated gases. Compared to the Phase I nominal acid runs with 10% of the projected noble metals, the amount of gases generated during the Phase II runs with nominal noble metals appeared to be much higher. No hydrogen and very little nitrous oxide were generated in the original Decant 9 run (SB3A-2).[1] Once again the results will be discussed in more detail in Section 6.0.

As mentioned earlier, supernate samples were removed at the end of acid addition to monitor the soluble species. These samples were also pulled during Phase I but were not analyzed. Due to the large difference in behavior seen between the two runs, the Mobile Lab analyzed all four samples to determine the soluble species. Both ICP-AES and IC analyses were performed and the results are given in Table 8 for both the Phase I and Phase II tests.

Table 8 – SRAT Slurry Supernate at the End of Acid Addition (mg/L)

Phase	Run ID	Al	Ba	Ca	Cu	Fe	Gd	K	Nitrite	Nitrate
II	SB3A-8	986	4.85	41.2	114	2800	2.71	496	231	36100
II	SB3A-9	721	2.16	74.2	119	521	2.44	688	177	27000
I	SB3A-1	1110	0.139	16.6	103	2130	0.550	549	3060	30300
I	SB3A-2	698	0.104	30.9	107	258	0.245	665	584	25800
Phase	Run ID	Mg	Mn	Na	Ni	Si	Zn		Formate	Oxalate
II	SB3A-8	96.2	2480	27700	5.92	40.6	29.2		43700	21200
II	SB3A-9	78.0	3200	24800	52.4	35.7	55.0		43400	5140
I	SB3A-1	30.1	1150	25900	5.40	47.6	3.05		41600	22700
I	SB3A-2	90.4	2310	23200	4.66	65.9	7.05		35900	6800

Note: SRAT slurry was sampled and sample was centrifuged. Supernate was decanted for analysis.

With the exception of Al, most of the sludge components that are usually considered insoluble were more soluble in the higher acid runs. Most cases were only 1.5 to 2 times greater, but in some instances solubility was ~10 times greater. Relative to the total amounts of each of the components present in the slurry, significant amounts of Cu, K, and Na were

soluble. Mg and Mn also were present in relatively high quantities. The supernate of the starting sludge was not measured in Phase II; however, the sludge simulant was the same as that used in the Phase I testing. Therefore, the soluble species in the initial sludge should be similar in this phase. All of the components, with the possible exception of K, were more soluble at the end of acid than at the beginning of the run. The anion data revealed that oxalate was not completely soluble, and was more soluble in the higher oxalate run. Nitrite in the supernate was much greater for the Phase I runs, which is consistent with the lower nitrite seen in the SRAT slurry samples for the SB3A-8 and SB3A-9 SRAT slurry samples taken at the end of acid addition. Formate and nitrate were completely soluble.

Although several problems were experienced with the laboratory equipment during the runs (see the description above), no significant processing issues were identified. Mixing and heating of the slurries during the SRAT/SME was not an issue. As alluded to in Section 4.0, a large amount of material was condensed in the FAVC during the Run SB3A-8 SRAT cycle. The condensed mass was ~45 g compared to the typical ~10 g normally seen. The condensed material was also darker in color than the typically clear to pale yellow condensed material. In addition to this high mass of material, both runs had significant generation of brown gas during the SRAT cycle acid addition. This gas permanently stained the line to the manometer. The cause for the differences will be explored in section 5.3 when results of the analyses are discussed. No problems with foaming or processing of the slurries were evident.

### 5.3 SRAT and SME Product Characterization

The SRAT product from each run was characterized for the anion concentration, cation concentration, solids content, density, and carbon concentration. The product anion concentration for each run is given in Table 9. Nitrate concentrations decreased very slightly from the last sample taken during SRAT processing and the SME product showed a slight concentration increase compared to the SME sample taken before frit addition started. Slight decreases in formate concentration were seen from the last sample to the SRAT product and for the SME sample and product. Oxalate concentrations slightly increased from the SRAT to the SME product. Compared to the oxalate results in Table 7, it would appear that the first results for SB3A-8 were correct and the second results for SB3A-9 were correct. In addition to analytical error, it is possible that the solubility of some of the species changed when the products cooled.

**Table 9 – SRAT and SME Product Anion Concentration (mg/kg)**

Anion	SB3A-8		SB3A-9	
	SRAT	SME	SRAT	SME
Nitrite	<100	<100	<100	<100
Nitrate	34,650	35,850	22,650	21,750
Formate	26,100	17,400	30,350	25,350
Oxalate	32,400	38,100	22,450	23,800

Note: Analyses performed on weighted dilution of two samples.  
Results represent an average of two measurements.

The results in Tables 4, 7, and 9, along with the known addition amounts of nitric acid and formic acid, were used to estimate the destruction that occurred during the SRAT and SME cycles. The SRAT receipt numbers are based on the feed that was in the vessel at the start of the runs. The results have been adjusted for the samples that were pulled before and during processing, and the samples' associated anions were considered removed from the system from a possible reaction standpoint. Hence, the receipt anion mass was adjusted by the amount of the anion removed with the samples when calculating the destruction that occurred during processing. The numbers given in Table 10 strictly convey total destruction based on the starting and ending parameters. They do not attempt to estimate the effect that the removed anions would have had on the system, to account for any conversion of nitrite to nitrate, or to incorporate other possible reactions occurring during processing. This will be discussed in more detail in Section 6.0. Since the SRAT product mass was not weighed, estimates for the associated SRAT product mass had to be made. This was done by assuming that 3% of the sludge receipt mass was lost during SRAT processing. The 3% loss number was based on the Phase I testing, and it is realized that mass loss may have been higher due to the greater amounts of acid used in the Phase II runs.

**Table 10 – Destruction of Nitrate, Formate, and Oxalate – SRAT Receipt Relative to SRAT Product and SRAT Product Relative to SME Product**

Parameter	SB3A-8	SB3A-9
SRAT Receipt Nitrate Mass (g) <sup>1</sup>	7.186	4.533
Nitrate Added (g)	82.50	61.39
Nitrate Removed in Samples (g) <sup>2</sup>	5.166	3.399
SRAT Product Nitrate Mass (g) <sup>3</sup>	89.05	58.84
<b>% Nitrate Destruction in SRAT<sup>4</sup></b>	<b>-5.63%</b>	<b>5.89%</b>
Formate Added in SRAT (g)	111.7	101.7
Formate Removed in Samples (g) <sup>2</sup>	4.407	4.655
SRAT Product Formate Mass (g) <sup>3</sup>	67.08	78.85
<b>% Formate Destruction in SRAT<sup>4</sup></b>	<b>37.48%</b>	<b>18.76%</b>
Initial Sludge Oxalate Mass (g) <sup>1</sup>	110.6	63.26
Oxalate Removed in Samples (g) <sup>2</sup>	5.541	3.242
SRAT Product Oxalate Mass (g) <sup>3</sup>	83.27	58.23
<b>% Oxalate Destruction in SRAT<sup>4</sup></b>	<b>20.72%</b>	<b>2.83%</b>
Nitrate Removed with SRAT Product and SME Samples (g) <sup>2</sup>	7.867	5.366
SME Product Nitrate Mass (g) <sup>3</sup>	68.19	45.09
<b>% Nitrate Destruction in SME<sup>5</sup></b>	<b>16.01%</b>	<b>15.69%</b>
<b>% Total Nitrate Destruction<sup>6</sup></b>	<b>11.05%</b>	<b>21.12%</b>
Additional Formate Added (g)	8.00	8.82
Formate Removed with SME Samples (g) <sup>2</sup>	5.855	7.158
SME Product Formate Mass (g) <sup>3</sup>	33.44	52.76
<b>% Formate Destruction in SME<sup>5</sup></b>	<b>51.69%</b>	<b>34.47%</b>
<b>% Total Formate Destruction<sup>6</sup></b>	<b>69.44%</b>	<b>46.56%</b>
Oxalate Removed with SME Samples (g) <sup>2</sup>	7.444	5.351
SME Product Oxalate Mass (g) <sup>3</sup>	73.23	49.34
<b>% Oxalate Destruction in SME<sup>5</sup></b>	<b>3.42%</b>	<b>6.86%</b>
<b>% Total Oxalate Destruction<sup>6</sup></b>	<b>24.96%</b>	<b>9.76%</b>

<sup>1</sup>Based on analyses given in Table 4 and sludge component mass in starting weight in Table A-2.

<sup>2</sup>Based on analyses given in Table 7 and sample weights in Table A-2. Formate values are an average of the two data points. Oxalate values for SB3A-8 are from the first sample, while values for SB3A-9 are from the second sample.

<sup>3</sup>Based on analyses given in Table 9 and estimated SRAT product weights and actual SME product weights given in Table A-2.

<sup>4</sup>Destruction represents difference of [SRAT product – (Receipt+added-removed in samples)] and the percent is calculated relative to (Receipt+added-removed in samples). “-” signs indicates a gain instead of loss.

<sup>5</sup>Destruction represents difference of [SME product – (SRAT product+added-removed in samples)].

<sup>6</sup>Total destruction represents the relative difference between the Receipt (adjusted for additions and samples removed) – SME product.

Nitrate difference in the SRAT was within analytical error ( $\pm 10\%$ ). However, small amounts of nitrate were destroyed during the SME. When the total nitrate destruction numbers are considered, SB3A-8 could still be within analytical error since the total was  $\sim 11\%$ , while it is apparent that some nitrate was destroyed during SB3A-9. This was the run that continued to generate nitrous oxide during the SME cycle so the destruction might be plausible. Another thing to remember is that some of the low or negative destruction may be the result of conversion of nitrite to nitrate. Very small changes in the amount of nitrate present were seen in the Phase I runs.[1] Formate was destroyed in significant amounts in both Phase II runs and during both the SRAT and the SME cycles. Total destruction was also significant with much more destroyed in Run SB3A-8 than Run SB3A-9. The very high destruction was surprising since levels this high had not been seen during previous SB3 runs. The other SRAT/SME runs performed with high acid and the nominal noble metals levels (Runs SB3-21 and SB3-23) only had total destruction on the order of  $\sim 50\%$ . [10] The formate destruction was also much higher than what was seen in the Phase I runs.[1] Oxalate destruction was different with the two runs and for the two process cycles. SRAT oxalate destruction was higher in both runs than in the SME. Once again, the Decant 5 run (SB3A-8) was higher than the Decant 9 run (SB3A-9). SRAT oxalate destruction was much higher for the Decant 5 run in this phase of testing than in the original phase of the testing, while the oxalate destruction for the Decant 9 runs was comparable.[1] Very small to insignificant quantities of oxalate were destroyed in the SME cycle. Compared to the previous SB3 SRAT/SME runs with nominal noble metals and excess acid (Runs

SB3-21 and SB3-23), Run SB3A-8's total oxalate destruction was ~3 times greater, while it was comparable for Run SB3A-9.[10] A more thorough discussion of the balance for the two runs will be given in Section 6.0.

As mentioned in section 3.3, oxalate and formate destruction values had to be assumed prior to calculating the acid split for redox balance. Only 30% total formate destruction was assumed, whereas 20% total oxalate destruction was assumed. Based on Table 10, formate destruction was under predicted by a factor of at least 2 for Run SB3A-8 and by a factor of 1.5 for Run SB3A-9. Oxalate destruction, on the other hand, was comparable for Run SB3A-8 and over-predicted for Run SB3A-9. In general, the under-prediction for formate destruction would cause the melter feed to be more oxidizing than predicted. Based on the SME product numbers given in Table 10, the analyzed Mn content in the SRAT products (given in Table 11 below), and the estimated amount of coal remaining in the sample, the predicted redox using Equation (2) for Run SB3A-8 would be 0.116 and for Run SB3A-9 would be 0.331. Based on the slope and intercept values recommended in the SB3 redox equation [5], the predicted redox for Run SB3A-8 would be 0.130 and 0.309 for Run SB3A-9. The SME product samples were melted in the dry melt rate furnace at ACTL. The results of the testing will be discussed in a separate memo.

As mentioned in Section 4.0, the SRAT and SME products were calcined at 1100°C in order to prepare them for cation analyses. The oxides detected in the calcined solids are given as Table 11.

**Table 11 – SRAT and SME Product Results (Calcined Solids Wt%)**

Oxide	SB3A-8		SB3A-9	
	SRAT	SME	SRAT	SME
Al <sub>2</sub> O <sub>3</sub>	15.2	5.40	18.2	6.78
B <sub>2</sub> O <sub>3</sub>	<0.100	5.09	<0.100	4.94
BaO	0.229	0.070	0.266	0.087
CaO	3.18	0.882	3.73	1.15
CuO	0.070	0.060	0.134	0.075
Fe <sub>2</sub> O <sub>3</sub>	32.5	10.9	38.7	13.5
Gd <sub>2</sub> O <sub>3</sub>	0.047	0.015	0.056	0.018
K <sub>2</sub> O	0.103	0.113	0.307	0.127
Li <sub>2</sub> O	0.138	4.48	0.141	4.40
MgO	0.279	1.57	0.358	1.57
MnO	5.44	1.86	7.01	2.33
Na <sub>2</sub> O	32.3	16.5	21.6	11.7
NiO	0.997	0.322	1.30	0.409
PbO	0.092	0.100	<0.001	0.014
SiO <sub>2</sub>	2.33	52.4	2.52	51.79
ZnO	0.372	0.120	0.438	0.157
ZrO <sub>2</sub>	0.607	0.209	0.729	0.266
<b>Totals</b>	93.88	100.09	95.49	99.31

Note: Two aliquots removed from product sample then calcined and analyzed.

Results represent an average of the two measurements.

Run SB3A-8 had a relatively low total oxide sum for the SRAT product, indicating poor recovery from the digestion and analyses. Typically, acceptable recovery is 100±5%. This problem has repeatedly been seen in the presence of sodium oxalate. It is possible that the sodium oxalate or other compounds that are forming in the presence of oxalate are not readily dissolved with the existing preparation method; therefore, lower total oxides or poorer recoveries would be seen. The oxide recoveries for the other samples were acceptable. When the SRAT product compositions are compared to the target SRAT feed compositions given in the associated run plans [11,12], some of the major sludge components are > ±10% from the target. Na, Ni, and Si were all present at less than target levels, which was consistent with the data reported in Table 3 for the initial sludge. Differences in the level of SiO<sub>2</sub> can be attributed to uneven distribution of the sand particles in the SRAT product and the difficulty in keeping the sand particles suspended in the slurry. The low Na is consistent with the lower than targeted oxalate levels seen in the starting sludge. If the target SRAT compositions are combined with the target frit composition and loading, then a few of the SME oxides were also > ±10% from the target. Both products were high in Mg and low in Ni. Run SB3A-8 SME product was also low in Mn, while Run SB3A-9 SME product was also low in Ca. Overall, the compositions represented a reasonable

estimation of SB3 simulant. Based on the SRAT and SME compositions given in Table 11 and the known Frit 202 composition, the target waste loading (i.e., 35 wt%) appeared to have been met.

The SRAT and SME products were also filtered to remove the supernate, so the soluble components could be determined. The supernate cation concentrations are given in Table 12.

**Table 12 – Filtered SRAT and SME Product Supernate (mg/L)**

Sample ID	Al	B	Ba	Ca	Cu	Fe	Gd	K	Li
SB3A-8 SRAT	6.13	2.14	0.664	0.274	57.5	1.00	3.92	634	1.26
SB3A-8 SME	0.314	58.9	0.219	1.74	35.4	1.93	0.57	1220	199
SB3A-9 SRAT	0.259	1.43	<0.10	<0.10	1.09	<0.10	<0.10	776	1.16
SB3A-9 SME	1.06	80.5	0.283	0.361	2.09	3.39	2.50	1380	328
Sample ID	Mg	Mn	Na	Ni	Si	Zn	Nitrate	Formate	Oxalate
SB3A-8 SRAT	62.1	1720	33700	221	44.0	43.2	41300	32900	26500
SB3A-8 SME	254	507	42300	343	105	3.14	50600	29300	50200
SB3A-9 SRAT	39.6	482	26600	6.07	68.2	<0.10	29900	39000	13200
SB3A-9 SME	321	1460	39300	242	85.9	1.95	32200	37100	22900

Note: Product supernate was filtered and then analyzed. Analysis was performed on one sample.

The cations that were most prevalent in the SRAT supernate included K, Mn, and Na. This is expected for K and Na since they are typically present as soluble salts. The relative amounts of Na in the SRAT product supernate were ~100% compared to the ~65% seen during the Phase I runs with the same decant compositions.[1] Substantial differences in the solubility of some of the cations (e.g., Cu, Ni, Zn, and Gd) were seen between the runs with the Decant 5 SRAT supernate having higher concentrations. In general, the relative amounts of soluble species were lower for the SRAT supernate than for the samples taken at the end of acid addition. Mn is expected to be present in the SRAT product supernate based on the assumed reactions occurring during the SRAT. However, large quantities of Mn have not been detected in the supernate during the previous runs with sodium oxalate.[10,15,16] For SB3A-8, ~30% of the Mn was soluble, while only ~6% was soluble for SB3A-9 SRAT product supernate. Both runs had more Mn soluble in the SRAT products than in the initial sludge, which supports the reduction of  $Mn^{+4}$  to  $Mn^{+2}$ . Very little Ca was detected in the supernate, which is consistent with previous SB3 runs containing sodium oxalate.[10,15,16] This is expected to be the result of Ca reacting with the oxalate from the added sodium oxalate. Generally speaking, the SME product supernate had fewer soluble metals/cations present. Most of the typical sludge components were relatively insoluble. K, once again, had the highest relative solubility. Na solubility was also relatively high but less than in the SRAT product. Ni was one of the few components whose relative solubility was greater in the SME product than in the SRAT product. Mn solubility was slightly decreased for Run SB3A-8, while it slightly increased for the SME product from Run SB3A-9. With respect to the anions, nitrate and formate were completely soluble, while the relative oxalate solubility increased compared to the SRAT products.

The total and dissolved solids were measured on the SRAT and SME products, and the insoluble and soluble solids were then calculated. As mentioned above, the calcined solids were also measured. To complete the physical property analyses, the slurry density and final pH were measured. The results are given in Table 13.

**Table 13 - Physical Property Data on SRAT and SME Products**

Sample ID	Total Solids	Insoluble Solids	Soluble Solids	Calcined Solids	Slurry Density (g/ml)	pH
SB3A-8 SRAT Product	19.9%	9.29%	10.7%	11.7%	1.18	8.27
SB3A-8 SME Product	51.7%	43.3%	8.41%	42.4%	1.49	8.31
SB3A-9 SRAT Product	20.5%	12.9%	7.52%	13.7%	1.16	8.47
SB3A-9 SME Product	50.9%	42.8%	8.09%	43.6%	1.41	8.70

Note: Measured on two aliquots from the same sample. Data reported is an average. Total and dissolved solids were actually measured and insoluble and soluble solids were calculated. The pH is measured at room temperature versus the pH measured at boiling in Figures 2 and 3, so is expected to change slightly.

The total solids were higher than the initial sludge possibly due to the loss seen during the SRAT cycle, but were consistent with the values seen for other SB3 simulant runs.[1,10,15] The SME target solids was 45% so the actual SME solids were slightly higher than targeted. This could potentially be the result of water lost or excess frit added during processing. The insoluble and soluble solids were different for each run. The values appeared to continue to be affected by the level of sodium oxalate present, with lower insoluble and higher soluble solids seen in the run with more sodium oxalate (i.e., Run SB3A-8). The SRAT results are consistent with previous SB3 simulant runs.[1,10,15]. The insoluble and soluble solids for the SME product were consistent between the runs. The reported calcined solids had a wide spread for the SRAT products, but were consistent with earlier runs. The calcined solids were close to the target for the SME products. Slight variation was seen in the measured slurry density from run to run, and the results were in line with previously reported slurry densities for the SB3 simulant runs.[1,10,15] The product pH measurements were performed after the testing was complete and showed slight variation, but were consistent with the pH measured during the runs. These numbers are slightly higher than what was seen at the end of the process, when the slurries were at elevated temperatures.

The carbon contents of the SME products were measured by ADS using methods developed for SB3. The results are reported in Table 14. As would be anticipated from SRAT processing, very little inorganic carbon was detected in any of the SME products. This confirms that the carbonates in the initial sludge have been reacted. The total carbon varied with the run, with the highest present in Run SB3A-8 containing the higher level of sodium oxalate. Both values appeared to be lower than anticipated, but they will be assessed in more detail in Section 6.0 when the overall carbon balance is performed.

**Table 14 – Carbon Analyses on the SME Products (µg/ml)**

Run ID	Total Carbon <sup>1</sup>	Inorganic Carbon <sup>1</sup>	Organic Carbon <sup>2</sup>
SB3A-8	5,040	70.7	4,969
SB3A-9	3,730	76.0	3,654

<sup>1</sup>Single analysis of the product where sample was ground to homogenize the coal.

<sup>2</sup>Not an actual measurement, difference of total carbon and inorganic carbon measurements.

As mentioned earlier, samples from the FAVC from the SRAT and the SME cycle, the MWWT from the end of both cycles, and the SMECT from SRAT processing were analyzed to ascertain what components might be causing the dramatic change in color. Both ICP-AES and IC were performed and the results are reported in Table 15. The pH of the samples was also measured and is given in the table. Once again, the FAVC samples were removed after the completion of the SRAT and the SME cycles and are labeled as such. The MWWT samples are from the end of the combined SRAT/SME cycle. The SMECT sample is from the dewater during the SRAT cycle. As a reminder, only the SRAT cycle was performed for the Phase I runs, so all samples are from the SRAT. Several species were below the detection limit of the analyses and are not included in the table. These included Ba, Fe, Gd, Li, Mg, Mn, Ni, and oxalate.

Table 15 – Analyses of FAVC, MWWT, and SMECT Samples

Species	SB3A-1 FAVC	SB3A-8 SRAT- FAVC	SB3A-2 FAVC	SB3A-9 SRAT- FAVC	SB3A-8 SME- FAVC	SB3A-9 SME- FAVC	SB3A-1 SMECT	SB3A-8 SMECT	SB3A-2 SMECT	SB3A-9 SMECT	SB3A-1 MWWT	SB3A-8 MWWT	SB3A-2 MWWT	SB3A-9 MWWT
<b>Al</b>	1.45	0.410	1.66	0.558	0.397	0.402	0.564	0.984	1.12	0.859	1.15	0.407	0.896	0.398
<b>B</b>	4.45	0.572	5.34	0.286	0.055	<0.150	0.113	2.02	2.27	1.68	2.66	0.013	1.98	<0.150
<b>Ca</b>	<0.060	<0.060	<0.060	<0.060	<0.060	<0.060	<0.060	2.99	<0.060	<0.060	<0.060	<0.060	<0.060	<0.060
<b>Cu</b>	0.188	0.085	0.116	0.093	0.091	0.080	0.091	0.102	0.093	0.086	0.082	0.114	0.081	0.097
<b>K</b>	2.03	1.44	2.27	1.44	1.42	1.49	1.41	1.80	1.83	1.70	1.82	1.40	1.71	1.41
<b>Na</b>	13.2	13.4	14.7	7.12	8.60	6.19	9.24	9.13	10.1	8.96	11.4	5.69	8.31	7.61
<b>S</b>	2.41	<1.00	<1.00	0.296	<1.00	<1.00	<1.00	<1.00	<1.00	<1.00	<1.00	<1.00	<1.00	<1.00
<b>Si</b>	95.5	121	123	176	99.1	22.2	84.7	195	116	224	63.4	46.9	66.2	36.7
<b>Zn</b>	3.87	<0.010	<0.010	<0.010	<0.010	<0.010	0.137	<0.010	<0.010	<0.010	<0.010	<0.010	<0.010	<0.010
<b>Nitrite</b>	<100	<100	<100	<100	520	344	<100	<100	<100	<100	<100	<100	<100	<100
<b>Nitrate</b>	310000	49300	51600	59600	10000	3880	7380	2100	1050	1130	265	<100	<100	<100
<b>Formate</b>	<100	162	156	<100	<100	<100	284	1670	209	741	<100	<100	439	<100
<b>pH</b>	<1.00	7.87	<1.00	8.54	9.19	9.35	<1.00	1.43	1.72	1.67	2.26	9.68	2.92	9.50

The data presented does not identify any significant differences that were thought to be attributed to the changes in color. Based on the GC data and this fact, it would appear that it was the overall amounts of gases generated that may have caused the discoloration as opposed to the gases actually condensed and sampled in the FAVC, MWWT, or SMECT. However, a few items of interest were identified. In the FAVC samples, more Na was present in the SRAT SB3A-9 FAVC than in the SB3A-2 FAVC. More Si was found in both the Phase II SRAT FAVC samples compared to the Phase I samples. The Si concentration decreased for the SB3A-9 SME FAVC sample but did not for the SB3A-8 sample. Al, Cu, and K were present in higher concentrations in the Phase I SRAT FAVC samples. This may possibly be the result of higher solubility of these components during processing, but the exact explanation is not known. B was not present during the SRAT so any differences are due to contamination or analytical error. S had mixed behavior with more present in Phase I for Decant 5, while the result for Decant 9 is unknown because of the detection limit utilized in Phase I. A very high concentration of nitrate was detected in the SB3A-1 FAVC. Since the reported value was ~10 times the level of any other FAVC sample, it was re-analyzed but the same results were obtained. No obvious explanation for this dramatic difference exists. The nitrate was greater in Run SB3A-9 than Run SB3A-8, while the SME samples were much lower than the SRAT samples. No nitrite was detected in the SRAT FAVC samples, but it was detected in the SME FAVC samples. This may support the nitrate destruction reported for the SME cycles since reactions had to be occurring to generate nitrite. Formate concentration was slightly higher in the SRAT FAVC samples from SB3A-8 than SB3A-9, while no formate was detected in the SME samples. Some formate was also detected in the Phase I run (SB3A-2) of Decant 9 and none was detected in the Phase II run (SB3A-9) of Decant 9. The pH of the Phase I FAVC samples were significantly different than the Phase II FAVC samples. The Phase I samples were highly acidic, whereas the Phase II samples were basic. No obvious explanation for this difference exists.

As to the SMECT samples, more Ca was detected in SB3A-8 than in SB3A-1 and SB3A-9. More Si was also detected in the Phase II runs than in the Phase I runs. Like the FAVC sample, the SB3A-8 SMECT sample also contained less nitrate. Formate, on the other hand, was greater in the SMECT samples from Phase II with Run SB3A-8 having a greater concentration than Run SB3A-9. The pH of the SMECT samples were similar and were all acidic.

Finally, the MWWT samples can not be compared on a totally equivalent basis since they were taken at different times of the chemical process cycle, but some similarities and differences can be seen. More Na and Si were detected in the MWWT samples from Phase I. No nitrate was detected in the Phase II MWWT samples, while a small amount was detected in the Phase I Decant 5 (SB3A-1) run. Similarly, no formate was detected in the Phase II MWWT samples, while a small amount was detected in the Phase II Decant 9 run (SB3A-2). The measured pH for the Phase II samples were once again much more basic than the Phase I samples. However, this is likely attributed to the SME cycles that were performed as part of the Phase II studies. Performing the SME cycles exposed the MWWT to more processing time and more flushes of water through the system (due to the decontamination canister additions and dewatering); therefore, the pH of the contents of the MWWT would have been affected.

Rheology testing was performed on the SRAT and SME products from both runs to determine any impacts of the sodium oxalate on rheology. The products were tested at the received total solids loading. The preliminary results indicated that the SRAT product from Run SB3A-8 had essentially the same up and down flow curves and was Newtonian in nature. The consistency for Run SB3A-8 SRAT product was determined to be 2.2 cP. The SRAT product from Run SB3A-9 also had the same up and down flow curve but was non-Newtonian in behavior. The yield stress for the Run SB3A-9 SRAT product was determined to be 5.4 dynes/cm<sup>2</sup> and the consistency was 3.65 cP. The preliminary results were consistent with the SRAT product results for the Decant 5 and Decant 9 runs in Phase I.[1] The SME products from both runs in Phase II had very different up and down curves. Two different samples of each product were run, and the results were consistent. It is believed that settling may have affected the SME product results. This will be further investigated once the SB3 or SB2/SB3 compositions are finalized. Complete details of the analyses will be documented and issued once the additional SB3 runs are completed since additional material, more closely matching the anticipated compositions, will be quantified from those runs.

## 6.0 MASS BALANCE CALCULATIONS

This section puts the material balance results for SB3A-8 and SB3A-9 into the same context as that done for the earlier SB3 simulant studies.[9,18] The primary purpose of constructing material balances was to understand the behavior of selected anions and key off-gas species during processing. Material balance analyses for the 24 4-L SRAT cycle

simulations using Tank 8 simulant were summarized in WSRC-TR-2003-00041[9]. A similar analyses was performed for the three SME cycle simulations with Tank 8 simulant.[17]

## 6.1 Overall Material Balances

Overall mass balances with respect to the mass of material removed and added to the process vessel for the Phase II runs are given in Appendix A as Table A-2. These include both the SRAT and SME cycles. Phase II overall mass balances closed to within about 200 grams on a liquid-solid basis (given a starting mass of ~2900 g and a SME product mass of ~2000 g). This loss amount is consistent with other SB3 runs when both a SRAT and SME cycle were performed.[9,10] This was similar to the three SB3-Tank 8 simulant tests that included a SME cycle.[17] The bulk of the material balance deficit was probably contained in the offgas non-condensable species (CO<sub>2</sub>, NO, NO<sub>2</sub>, N<sub>2</sub>O, and H<sub>2</sub>). The remainder was measurement error and lost water vapor.

As mentioned earlier, the SRAT product mass in both runs was not measured before the start of the SME cycle. Therefore, an estimate of the SRAT product mass was required in order to study the SRAT and SME separately. Table A-2 gives a running balance of the masses added and removed from the vessel starting with the initial sludge addition. A similar balance was constructed backwards in time from the weighed mass of the final SME product. When the SME product numbers are compared to the running balances, the numbers indicate that overall material balance closure is within about 200 grams. The actual SRAT product mass was expected to lie between the calculated results from the two running balance methods. Furthermore, the SRAT product mass was expected to lie closer to the mass working backwards from the SME product mass than to the mass working forwards from the starting sludge. The reason for this was that roughly 70-80% of the measured off-gas mass was evolved during the SRAT cycle. The estimated SRAT product mass for both SB3A-8 and SB3A-9 was a weighted average using 80% of the SME product-based mass balance estimate and 20% of the starting sludge-based mass balance estimate. This gave SRAT product masses of 2564.9 g for Run SB3A-8 and 2513.4 g for Run SB3A-9.

Three balances were performed based on Al, Fe, and Mn to check the overall material balance. The iron and aluminum balances closed to within 5% from the initial sludge to the SME product. The errors were in the opposite directions for the two species in each balance indicating that the SME product mass relative to the starting sludge mass was essentially correct. The manganese balances closed to within 10-15%. Both products were low in manganese relative to the starting sludge. The reason for this is not clear. The weighted average SRAT product mass could be 3% low based on the iron and aluminum balances relative to the starting sludge mass. This was considered close enough to proceed to the carbon and nitrogen species balances.

## 6.2 Carbon Balances

### 6.2.1 Overall Carbon Material Balances

An overall carbon balance was developed to assess the magnitude of analytical uncertainty before studying individual oxalate, formate, and carbon dioxide species balances. Balances were constructed for the SRAT cycle, the SME cycle, and for the combined SRAT and SME cycles. Good closure on the carbon balance has permitted a reasonably reliable examination of the concentration changes of formate and oxalate ions during the SRAT cycle, as well as an assessment of the sources of carbon dioxide gas generation.

Carbon entered the SRAT in the form of carbonate ion, oxalate ion, coal, formic acid, and antifoam. Carbon species were lost during SRAT processing due to small samples and carbon dioxide gas generation. Two significant slurry samples were pulled after the SRAT cycle was complete. The remainder of the SRAT product slurry became the input for the SME cycle. Additional carbon entered the SME in the form of antifoam and as the formic acid associated with frit slurry additions. Carbon left the SME in the form of carbon dioxide gas and small samples.

Table 16 summarizes the carbon balance input terms for the SRAT cycle, SME cycle, and the combined SRAT/SME cycle, or "overall" simulation. The numbers are all given as pounds of carbon at DWPF scale (6000 gallons of fresh sludge at ~18 wt. % total solids). The SRAT scale factor between the ~2.5 liter slurry test and 6000 gallons was 1/9165. A smaller scale factor could be used for the SME cycle conversions, since mass was removed during and after the SRAT cycle. This would cause the mass out in the overall balance (based on the SRAT scale factor) to be different from the mass out in the SME balance (based on the SME scale factor). The SB3A-8 SME scale factor would have been

about 1/11,200 for a 6000 gallon batch of SRAT product at 20 wt. % total solids. To convert the SB3A-8 SME cycle numbers in the tables to this basis, it would be necessary to multiply them by 11,200/9165. The SB3A-9 scale factor would have been about 1/10,400 on the same basis. To convert the SB3A-9 SME cycle numbers to the 6000 gallon basis would require multiplying them by 10,400/9165. Using the different scales would make reading the tables more confusing; therefore, the SRAT scale factor was used for all conversions from the bench-scale to DWPF-scale.

Not all quantities in the total carbon balance were determined analytically, e.g. coal and the carbon mass of antifoam. Analytical methods to selectively track coal and antifoam either do not presently exist or have not been used on simulant samples. Known masses of coal and antifoam were added to each test. In Table 16, the numbers shown for coal and antifoam represent calculated values assuming perfect mixing and no reactions. The formate numbers were based on a titration of the formic acid and an accurate measurement of the volume added. Oxalate values were based on analyses of the starting Decant 5 and 9 sludges. The "Total In" column is the sum of all of the individual inputs.

**Table 16 – "Carbon In" Scaled to 6000 Gallons at 18 wt. % Total Solids (lbs)**

RUN	TIC	Coal <sup>1</sup>	Formate	Oxalate	Antifoam <sup>2</sup>	Total In <sup>3</sup>
SB3A-8 SRAT	60.6	45.8	602.0	609.3	15.2	1332.8
SB3A-8 SME	0.0	37.9	382.2	417.9	15.6	853.6
SB3A-8 Overall	60.6	45.8	644.5	609.3	17.3	1377.5
SB3A-9 SRAT	57.6	63.7	548.1	348.6	15.2	1033.2
SB3A-9 SME	0.0	52.7	421.0	262.5	15.6	751.8
SB3A-9 Overall	57.6	63.7	595.0	348.6	17.3	1082.3

<sup>1</sup>Coal is a calculated number based on the amount added

<sup>2</sup>Antifoam is a calculated number based on the amount added

<sup>3</sup>Total in reflects summed values in an excel spreadsheet, some round-off is accounted for in the total.

Table 17 gives the corresponding set of carbon masses in the various exit streams. Formate and oxalate are based on analyses of the products. The samples represent all carbon removed from the system in samples and includes formate, oxalate, coal, and antifoam.

The CO<sub>2</sub> mass flow-rate was determined using the GC data presented in subsection 5.2 combined with the flow-rate of the helium internal standard. The air purge flow is reduced in the SME cycle compared to the SRAT flow-rate. The CO<sub>2</sub> mass flow-rate was integrated over the time of the SRAT cycle to give the total mass of CO<sub>2</sub> evolved. Equation (3) was used to calculate CO<sub>2</sub> mass flow-rate.

$$\text{Eq (3)} \quad CO_2, g / \text{min} = (\text{He flow, sccm}) * \left( \frac{\text{vol\% } CO_2}{\text{vol\% He}} \right) * \left( \frac{44.01 g / \text{gram-mole}}{22,415 \text{ scc} / \text{gram-mole}} \right)$$

where sccm is standard cubic centimeters per minute. A CO<sub>2</sub> flow-rate was obtained for each GC reading, i.e. about every three minutes. The total mass of CO<sub>2</sub> evolved during any portion of the simulation was determined by integrating the instantaneous flow-rates over the time period of interest, per Equation 4.

$$\text{Eq (4)} \quad CO_2, g = \int_{t_1}^{t_2} CO_2, g / \text{min} dt$$

where t is time, and t<sub>1</sub> and t<sub>2</sub> are the beginning and ending times of the portion of the simulation of interest. The indicated integration was made numerically, since the available flow-rates were in the form of discrete time data. Simpson's rule was used to perform the numerical integration. The integration across three consecutive flow-rate determinations takes the form given in Equation 5:

$$\text{Eq (5)} \quad CO_2, g, \text{ from } t_i \text{ to } t_{i+2} = \frac{(t_{i+2} - t_i)}{6} * \left( \frac{CO_2, g}{\text{min at } t_i} + 4 * \frac{CO_2, g}{\text{min at } t_{i+1}} + \frac{CO_2, g}{\text{min at } t_{i+2}} \right)$$

where the t<sub>i</sub> are the times associated with the three consecutive flow-rate determinations. These masses are then summed to evaluate the integral above. Two sums are obtained, one for i taking on odd values, and one for i taking on even values. These two sums are checked against each other, and then averaged to obtain the mass of CO<sub>2</sub> evolved over

a given period of time. Agreement has always been very good. (The time periods of interest were generally much, much longer than three minutes, so having one term more or less in a given sum was of little consequence to the total.)

**Table 17 – “Carbon Out” Scaled to 6000 Gallons at 18 wt. % Total Solids (lbs)**

RUN	Coal <sup>1</sup>	Formate	Oxalate	Samples	CO <sub>2</sub> <sup>2</sup>	Anti-foam <sup>3</sup>	Total Out <sup>4</sup>
<b>SB3A-8 SRAT</b>	41.3	363.2	447.8	52.0	354.9	13.7	1273.0
<b>SB3A-8 SME</b>	37.5	199.0	387.7	3.6	71.1	15.4	714.4
<b>SB3A-8 Overall</b>	37.5	199.0	387.7	112.9	426.0	15.4	1178.5
<b>SB3A-9 SRAT</b>	57.5	402.5	282.9	47.4	313.0	13.7	1117.1
<b>SB3A-9 SME</b>	52.2	284.7	249.7	3.7	76.9	15.4	682.6
<b>SB3A-9 Overall</b>	52.2	284.7	249.7	105.1	389.9	15.4	1097.0

<sup>1</sup>Coal is a calculated number based on the amount added and estimated amount removed in samples

<sup>2</sup>CO<sub>2</sub> is calculated from an integration of the GC data.

<sup>3</sup>Antifoam is a calculated number based on the amount added and the estimated amount removed in samples

<sup>4</sup>Total out reflects summed values in an excel spreadsheet, some round-off is accounted for in the total

Table 18 summarizes the material balance closure for the runs. It incorporates the “total in” and “total out” columns from Table 16 and Table 17, respectively.

**Table 18 - Closure of the Overall Carbon Balance**

RUN	Total Carbon In (lbs)	Total Carbon Out (lbs)	Closure*
<b>SB3A-8 SRAT</b>	1332.8	1273.0	-4.5%
<b>SB3A-8 SME</b>	853.6	714.4	-16.3%
<b>SB3A-8 Overall</b>	1377.5	1178.5	-14.4%
<b>SB3A-9 SRAT</b>	1033.2	1117.1	8.1%
<b>SB3A-9 SME</b>	751.8	682.6	-9.2%
<b>SB3A-9 Overall</b>	1082.3	1097.0	1.4%

\*Closure was defined as  $\{100\% * (\text{carbon out} - \text{carbon in}) / (\text{carbon in})\}$  for the indicated run cycle (SRAT, SME, or overall)

Coal and antifoam account for about 10% of the material balance, and their treatment was theoretical. The rest of the overall carbon balance was derived from measured quantities, either masses or analytical measurements. Closure of the carbon material balance was not as good as was hoped for Run SB3A-8. The trend has been to have most SRAT cycles close with an error of +2% to +9%. As mentioned in subsection 5.1, some problems with the helium MKS flow controller were experienced during the addition of nitric acid in Run SB3A-8. An alternate flow controller was installed, but problems persisted with establishing the appropriate helium to air ratio for ~8 hours. It is possible that some CO<sub>2</sub> was evolved during this period and not accounted for in the material balance.

Neither SME cycle carbon balance closed particularly well. This was investigated thoroughly, but no definitive answer was obtained. The closure error reflects the following feature in both cases. The amount of formate lost, as determined by the overall mass balance and the IC data, was roughly twice the amount of carbon dioxide evolved. As stated in subsection 5.2, SRAT and SME product samples were re-analyzed by IC. Reproducibility of oxalate results remains an issue, but formate results were generally reproduced fairly well. Variations of over 30% were found in some of the oxalate results when samples were re-analyzed. These large changes could be due to instrument issues, but they could also be due to instability of oxalate in some of the samples themselves. The GC data received similar scrutiny. The evolved CO<sub>2</sub> masses were similar to those reported for SB3-21 and SB3-23. These were the two previous SME cycles with 100% of the nominal noble metal concentrations using Tank 8 simulant. Species balances on oxalate, formate, and CO<sub>2</sub> will be discussed in turn below. Some “what if” scenarios related to the closure errors are discussed at the end of the carbon dioxide species balance section below.

### 6.2.2 Oxalate Species Material Balance

Table 19 presents the oxalate species material balance data on a DWPF scale from the two runs. Oxalate comprised about one-third of the total carbon content of the sludge. The initial oxalate mass was calculated from the mass of

Decant 5 or Decant 9 simulant sludge added to the kettle combined with the analytical IC measurement. The oxalate in the SRAT product was calculated from the SRAT product oxalate IC data and the overall material balance estimate of the SRAT product mass. The oxalate in the SME product was calculated from the weighed mass of SME product combined with the SME product oxalate IC data. SRAT and SME scaling was made using the same assumptions that were used for the overall carbon balance tables above.

**Table 19 - Oxalate Balance Scaled to 6000 Gallons at 18 wt. % Total Solids**

RUN	Initial Oxalate <sup>1</sup> (lbs)	Final Oxalate <sup>1</sup> (lbs)	Oxalate to Samples <sup>2</sup> (lbs)	Gross Oxalate Lost (lbs)	% Oxalate Lost <sup>3</sup>
SB3A-8 SRAT	2234	1642	91	501	22.4%
SB3A-8 SME	1532	1421	7	104	6.8%
SB3A-8 Overall	2234	1421	208	605	27.1%
SB3A-9 SRAT	1278	1037	64	177	13.9%
SB3A-9 SME	962	916	6	41	4.2%
SB3A-9 Overall	1278	916	144	218	17.1%

<sup>1</sup>Determined from the IC analyses and the overall material balance

<sup>2</sup>Calculated from the SRAT and SME process slurry IC analyses (average of the oxalate results reported) and the associated sample masses

<sup>3</sup>Represents the gross oxalate loss relative to the initial oxalate

The gross oxalate loss was the initial oxalate mass minus the oxalate masses in the samples and the product. Slightly different losses are reported in this table compared to Table 10 because of differences in the mass estimates for the SRAT product and the IC values used for the samples. SRAT losses ranged from 14-22% of the initial oxalate added. Numerically significant losses of oxalate also occurred in 17 of the 18 Tank 8 tests with oxalate [18] and two of the three Phase I flowsheet tests with oxalate [4]. SRAT oxalate losses exceeded SME oxalate losses. This has been the general trend in the runs to date. SME oxalate losses in most cases have been near the noise level of the data [17], indicating that the SME cycle oxalate loss may be negligible. An overall loss of 20% of the initial oxalate was assumed in the pre-run calculations used to split the total acid addition requirement between nitric and formic acid for redox control. Measured loss results were approximately as anticipated.

### 6.2.3 Formate Species Material Balances

Table 20 gives similar species material balance information for the formate ion. The result is the net formate lost. It is the net loss because formate was both created and destroyed during processing. "Formate added" is the formate content of the formic acid addition to the SRAT and/or the frit formic acid addition to the SME. The starting sludge was free of formate. Formate in the samples and product were calculated from IC results during the run (average of the values reported in Table 7) coupled with the overall material balance masses for the SRAT and SME products. Two large samples were pulled between the SRAT and the SME cycle that shows up in the overall balances but not in the SRAT and SME cycle balances. Scaling to 6000 gallons was done in a consistent manner to that described above for the overall carbon balance and the oxalate species balance.

**Table 20 - Formate Balance Scaled to 6000 Gallons at 18 wt. % Total Solids**

RUN	Formate Added <sup>1</sup> (lbs)	Final Formate <sup>2</sup> (lbs)	Formate to Samples <sup>2</sup> (lbs)	Net Formate Lost (lbs)	% Formate Lost <sup>3</sup>
SB3A-8 SRAT	2257	1362	80	815	36.1%
SB3A-8 SME	1433	746	4	683	47.6%
SB3A-8 Overall	2417	746	173	1498	62.0%
SB3A-9 SRAT	2055	1509	84	462	22.5%
SB3A-9 SME	1579	1068	5	506	32.0%
SB3A-9 Overall	2231	1068	196	968	43.4%

<sup>1</sup>Calculated from the volume of formic acid added and the molarity of the solution

<sup>2</sup>Determined from the IC product and process slurry analyses and the overall material balance

<sup>3</sup>Represents the net formate loss relative to added formate.

The formate losses for both runs were quite significant. They exceed the pre-run loss estimates of 30% that were used to balance the total acid between nitric acid and formic acid. For both runs, this would have resulted in less formic acid being added than required to maintain the predicted redox (given all other input variables remained the same). Had this been the only variable changed or assumed incorrectly, more hydrogen would have likely been generated during each run. As discussed earlier, issues exist with the closure of the two SME cycle carbon balances. The tabulated SME cycle formate losses could be significantly overstated based on the observations of evolved carbon dioxide.

If the assumption is valid that the lost oxalate is converted into formate and carbon dioxide, then it is worth constructing a table where the lost oxalate from Table 19 is converted to formate and added to the net formate loss from Table 20. This estimate of a gross formate loss is given in Table 21. The Decant 5 and Decant 9 data for 10% nominal noble metals and relatively low total acid are given for comparison, SB3A-1 and SB3A-2, respectively. The physical significance of the “gross formate loss” is that it should be a better measure of formate ion that is destroyed by chemical reduction reactions than the net formate loss given in Table 20. The idea is  $IN - OUT + FORMED - LOST = 0$ . Table 20 calculated  $IN - OUT$  for formate. Table 19 is used to estimate the FORMED term (formed from oxalate), permitting a preliminary calculation of the LOST term. The LOST formate (gross formate loss) is presented in Table 21. Formate formed from oxalate was calculated by  $(45/88) * (\text{gross oxalate lost from Table 19})$ .

The present DWPF SRAT reaction formate consumption calculation is given by Equation 6.

$$g \text{ reaction formate} = (0.4 * \text{moles Mn} + 0.25 * \text{moles NO}_2^- + \text{moles Hg}) * 45.01 \quad \text{Eq (6)}$$

The result was then scaled like the other quantities in the carbon balance. It is shown in the final column of Table 21 for comparison to the gross reaction formate consumption calculated from the formate and oxalate species material balances, above and in WSRC-TR-2003-00132 [18]. Results for the Phase I Flowsheet Study 4-L SRAT runs with Decant 5 and Decant 9 sludges are shown for comparison. The acid stoichiometry is based on the new acid addition equation derived for SB3 [4] and is given for comparison.

**Table 21 - Gross Formate Loss from Consumption Reactions**

RUN	Noble Metals, % of Nominal	Acid, % Stoich.	Formate Made from Gross Oxalate Lost (lbs)	Net Formate Lost, (lbs)	Gross Formate Loss (lbs)	DWPF Reaction Formate (lbs)
SB3A-1	10%	95% <sup>1</sup>	(-15)	48	33	208
SB3A-8 SRAT	100%	125%	256	815	1072	220
SB3A-2	10%	110%	98	43	141	162
SB3A-9 SRAT	100%	135%	91	462	553	168

<sup>1</sup>A different acid addition equation was used in Phase I and the stoichiometry was 100%. The acid stoichiometry was recalculated with the new SB3 equation [4] and the results are presented here.

Although there have been many opportunities to accumulate analytical and material balance errors in reaching this point, there is clearly an enormous difference between processing at low acid-low noble metals versus high acid-high noble metals. This difference was most evident in the net and gross formate loss columns. These numbers increased dramatically with the increases in noble metal concentrations and total acid. No corresponding increase was seen for the anticipated reaction formate requirement. The additional lost formate was apparently entirely converted into carbon dioxide plus either hydrogen or water.

#### 6.2.4 Carbon Dioxide Species Material Balances

Table 22 compares the identified sources of carbon dioxide to the measured production rate of carbon dioxide as determined from the GC data as described above. The scaling to DWPF was identical to that used for the overall carbon balance and other carbon species balances above. The “% Error” column was calculated using Equation 7.

$$\text{Eq (7)} \quad \% \text{ Error} = \{(\text{CO}_2 \text{ evolved} - \text{sum of CO}_2 \text{ formation reactions}) / (\text{CO}_2 \text{ evolved})\} * 100\%$$

CO<sub>2</sub> evolution came from oxidation of formate and oxalate, hydrogen generation from formate, acidification of carbonate, and reduction reactions (denitrification, denitration, and metal reduction reactions collectively referred to as the

“reaction formate” loss). Only the reduction reaction extent term (the reaction formate loss) in Table 22 was not directly measured.

**Table 22 - CO<sub>2</sub> Balance Scaled to 6000 Gallons at 18 wt. % Total Solids**

RUN	CO <sub>2</sub> produced as C <sup>1</sup> (lbs)	C from sludge TIC <sup>2</sup> (lbs)	C from oxalate oxidation <sup>3</sup> (lbs)	C from HCOOH oxidation (lbs)	C from H <sub>2</sub> Generation <sup>4</sup> (lbs)	C from Reaction HCOOH (lbs)	Sum of C from sources (lbs)	% Error
SB3A-8 SRAT	354.9	60.6	68.3	154.3	21.0	64.8	369.0	-4.0
SB3A-8 SME	71.1	0.0	14.2	179.1	2.1	0.0	195.4	-174.5
SB3A-8 Overall	426.0	60.6	82.5	333.4	23.1	64.8	564.3	-32.5
SB3A-9 SRAT	313.0	57.6	24.2	95.5	14.5	13.8	205.6	34.3
SB3A-9 SME	76.9	0.0	5.6	119.1	9.6	0.0	134.3	-74.6
SB3A-9 Overall	389.9	57.6	29.8	214.6	24.1	13.8	339.9	12.8

<sup>1</sup>From GC analyses

<sup>2</sup>All initial sludge TIC was assumed to be converted into CO<sub>2</sub>

<sup>3</sup>All oxalate loss was assumed to be by wet air oxidation to formate and CO<sub>2</sub>

<sup>4</sup>GC hydrogen generation data was used to calculate the associated CO<sub>2</sub> evolution

This data set had the largest closure variations of the various individual carbon species balances. The SME cycle closure was related to a significant discrepancy between moles of formate lost relative to the moles of carbon dioxide evolved.

The SB3A-8 carbon dioxide error tracked the overall carbon balance error trend of small in the SRAT, high in the SME, and less high overall in Table 22. A 63% increase in the SME product formate mass determined from the IC result and overall mass balance would be necessary to bring the SME CO<sub>2</sub> balance into agreement. This would leave the overall CO<sub>2</sub> balance with a -4% error. This would also leave the overall SME carbon balance with a -1.8% error (instead of -16.3%) and the overall carbon balance with an error of -5.4% (instead of -14.4%). The overall formate loss during the SRAT/SME processing would fall from the 62% shown in Table 20 to 43% in this case. Re-analysis of the SME product formate, however, did not indicate any significant analytical error. The formate loss was probably in the 43-62% range for the processing conditions of Run SB3A-8, but a stronger statement cannot be made from the available data.

The Run SB3A-9 carbon dioxide error also tracked the overall carbon balance error trend of high in the SRAT, low in the SME, and close to balanced overall. A 22% increase in SME product formate over the IC-material balance value would be needed to balance the carbon dioxide in Run SB3A-9. This would change the overall carbon balance error for Run SB3A-9 to +7.1% and the SME carbon balance error to -1.2% in Table 18. (Small positive carbon balance errors have been the norm in the work prior to the Phase II runs.) This suggests that the formate loss may lie somewhere between the 43.4% from Table 20 and 33% after adjusting product formate mass to reconcile the carbon dioxide balance.

Table 23 breaks down the carbon dioxide evolved during the SRAT cycle and the eight distinct phases of the SME cycle. Numbers were scaled to DWPF using a factor of 9165.

Total carbon dioxide evolution in Run SB3-21 (75% remaining sodium oxalate) and SB3-23 (25% remaining sodium oxalate) SME cycles were 431 and 155 lbs. at DWPF scale respectively.[17] The totals are quite comparable. There was a larger jump in carbon dioxide generation associated with the frit additions in those two earlier runs. This was attributed to those runs having only two frit additions, each containing 50% of the total frit and accompanying formic acid. The Phase II runs added one-third of the total frit and accompanying formic acid in each of three separate additions.

**Table 23 - Carbon Dioxide Mass Evolved in SME Cycle Phases at DWPF Scale (lbs)**

	<b>SB3A-8</b>	<b>SB3A-9</b>
<b>Total SRAT CO<sub>2</sub> Evolution</b>	1301	1148
Dewatering after:		
Canister Water Addition 1	51	27
Canister Water Addition 2	41	34
Canister Water Addition 3	30	32
Canister Water Addition 4	25	37
Canister Water Addition 5	16	28
Frit Slurry Addition 1	29	38
Frit Slurry Addition 2	31	41
Frit Slurry Addition 3	37	41
<b>Total SME CO<sub>2</sub> Evolution</b>	260	278

### 6.2.5 Hydrogen Generation Relative to Carbon Dioxide Generation

Hydrogen mass generated in each phase of the SRAT and SME cycle was calculated in a similar manner to that used for carbon dioxide and nitrous oxide. Table 24 gives the results for the SRAT and the eight phases of each of the SME cycles. A scale factor of 9165 was used to convert all bench-scale results to DWPF scale. Raw GC data was plotted in subsection 5.2

**Table 24 - Hydrogen Mass Evolved at DWPF Scale (lbs)**

	<b>SB3A-8</b>	<b>SB3A-9</b>
<b>Total SRAT H<sub>2</sub> Evolution</b>	3.54	2.45
Dewatering after:		
Canister Water Addition 1	0.08	0.15
Canister Water Addition 2	0.06	0.21
Canister Water Addition 3	0.04	0.20
Canister Water Addition 4	0.03	0.23
Canister Water Addition 5	0.02	0.17
Frit Slurry Addition 1	0.03	0.23
Frit Slurry Addition 2	0.04	0.22
Frit Slurry Addition 3	0.05	0.18
<b>Total SME H<sub>2</sub> Evolution</b>	0.35	1.59

These SME hydrogen generation masses were similar to those for Runs SB3-21 (75% remaining sodium oxalate) and SB3-23 (25% remaining sodium oxalate). These were the two Tank 8 simulant SME cycle simulations with 100% nominal noble metals [10]. Total SME cycle hydrogen masses were 1.02 pounds and 0.32 pounds for Runs SB3-21 and SB3-23 respectively. Run SB3-23 had less excess acid than Run SB3-21, while Run SB3A-8 had more excess acid than SB3A-9. The four runs, ranked in terms of increasing excess acid, were SB3-23, SB3A-9, SB3-21, and SB3A-8. The total DWPF-scale SME hydrogen masses generated were 0.32, 1.59, 1.02, and 0.35 pounds respectively.

The explanation for the variations in hydrogen generated appears to be as follows. When a large excess of acid is present in the SRAT, the hydrogen generation is primarily in the SRAT. The tendency to produce hydrogen in the SME is mitigated by the vigorous reaction in the SRAT. When a modest excess of acid is present in the SRAT, the hydrogen generation rate in the SRAT is smaller. The tendency to produce hydrogen in the SME, however, remains small. At some amount of excess acid in-between these two cases, a significant amount of hydrogen generation is delayed from the SRAT cycle into the SME cycle. Little time is spent between the SRAT and the SME in this simulant work. Considerably more time is spent between the SRAT and the SME in DWPF. It is possible that catalyst poisoning reactions might be on-going while the SRAT product samples are being analyzed that would tend to negate this effect.

Therefore, the DWPF would be less likely to see the higher hydrogen levels in the SME that have been experienced in SRTC lab-scale testing.

Table 25 looks at the fraction of carbon dioxide generation that is interrelated with hydrogen generation. The assumption is that one mole of formic acid produces one mole of hydrogen and one mole of carbon dioxide.

**Table 25 - Carbon Dioxide Generation Associated with Hydrogen Generation (lbs)**

Run	CO <sub>2</sub> at 1:1 with H <sub>2</sub>	Total CO <sub>2</sub> measured	Net CO <sub>2</sub> not due to H <sub>2</sub>
SB3A-8 SRAT	77	1301	1224
SB3A-8 SME	7.6	260	252
SB3A-9 SRAT	53	1148	1095
SB3A-9 SME	35	278	243

The masses in Table 25 indicate that catalytic hydrogen generation (formic acid decomposition) accounts for only 6% of the observed carbon dioxide generation overall. The sources of SRAT carbon dioxide were discussed above in the carbon dioxide species balance (subsection 6.2.4). The SME cycle carbon dioxide generation not due to hydrogen can be attributed either to denitration reactions that produce CO<sub>2</sub> and/or to catalytic wet air oxidation (CWAO), which produces carbon dioxide and water, rather than carbon dioxide and hydrogen. Discussion and references on CWAO can be found in WSRC-TR-2003-00041 [9]. CWAO can produce carbon dioxide from either formic acid or oxalic acid.

### 6.3 SB3 Simulant Nitrogen Balances

Nitrogen containing species were tracked for nitrite ion destruction, nitrate ion concentration versus time, and N<sub>2</sub>O as a gas phase component. The primary reason for analyzing the nitrogen species data was to attempt to estimate the proportion of nitrite destruction by each of the three identified routes discussed in WSRC-TR-2003-00118 [4]: conversion to NO (and on to NO<sub>2</sub> or N<sub>2</sub>O<sub>4</sub>), conversion to N<sub>2</sub>O, and conversion to nitrate.

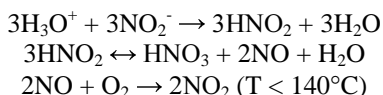
Table 26 gives a nitrate balance for the runs that was used to calculate the % of nitrite that was converted to nitrate. The nitrate masses are scaled in the same manner as the carbon masses discussed earlier. The inferred gain in SRAT cycle nitrate (negative nitrate loss in Table 26) is 100% attributed to the conversion of nitrite to nitrate. Table 26 also gives an overall nitrate balance and a nitrate balance for the SME cycle. This is not related to nitrite destruction, since all nitrite was destroyed in the SRAT cycles.

**Table 26 - Nitrate Balance Scaled to 6000 Gallons at 18 wt. % Total Solids**

RUN	NO <sub>3</sub> <sup>-</sup> in starting slurry (lbs) <sup>1</sup>	NO <sub>3</sub> <sup>-</sup> in as HNO <sub>3</sub> (lbs)	NO <sub>3</sub> <sup>-</sup> in product (lbs) <sup>1</sup>	NO <sub>3</sub> <sup>-</sup> to samples (lbs) <sup>1</sup>	NO <sub>3</sub> <sup>-</sup> Total In-Out (lbs)	% NO <sub>2</sub> <sup>-</sup> converted to NO <sub>3</sub> <sup>-</sup> (moles)
SB3A-8 SRAT	144.8	1666.9	1826.4	95.1	-109.8	16.5
SB3A-8 SME	1645.2	0.0	1382.5	7.2	255.5	-
SB3A-8 Overall	144.8	1666.9	1382.5	283.5	145.7	-
SB3A-9 SRAT	88.9	1240.4	1168.7	56.9	103.7	0
SB3A-9 SME	1084.3	0.0	927.2	4.2	152.9	-
SB3A-9 Overall	88.9	1240.4	927.2	145.5	256.6	-

<sup>1</sup>Based on IC analyses and overall mass balance.

The presence of oxalate seems to have interfered with the conversion of nitrite to nitrate in the SRAT based on the species balance results. About 30% would have been expected based on general non-oxalate historical SRAT data. The % nitrite converted to nitrate above only indicates the one nitrate mole formed, not the three nitrite moles consumed by the stoichiometry below.



The SRAT data for Run SB3A-8 indicate that nitrite was converted to nitrate. The SME and overall balances suggest that this may be a small analytical error. If very little nitrate was formed in the SRAT, then the indicated nitrate loss in the SME would become less. This would be closer to the expected behavior, which is that nitrate is fairly inert late in the SRAT and all through the SME cycles.

The SRAT data for Run SB3A-9 indicate that nitrate destruction exceeded nitrite to nitrate conversion (positive number in the second to last column), but this conclusion is not consistent with past observations. Instead, it seems more likely that only a negligible amount of nitrate was formed, no nitrate was lost, and there was a small analytical error of about 9% in the SRAT product nitrate. One alternative is an actual loss of nitrate by denitration in the SRAT. This has not been the typical result seen in the 18 Tank 8 SRAT runs with oxalate or the four SB3 Phase I flowsheet runs.[9,18] If denitration is occurring in the SRAT, then the % nitrite to nitrate conversion is being underestimated. This would complicate the analysis of the acid stoichiometric requirement for nitrite destruction.

Table 27 gives the N<sub>2</sub>O generated in the various phases of the two runs.

**Table 27 - Nitrous Oxide Mass Evolved at DWPF Scale (lbs)**

	SB3A-8	SB3A-9
<b>Total SRAT N<sub>2</sub>O Evolution</b>	52.9	28.8
Dewatering after:		
Canister Water Addition 1	2.1	0.8
Canister Water Addition 2	0.9	1.2
Canister Water Addition 3	0.02	1.3
Canister Water Addition 4	0	1.4
Canister Water Addition 5	0	0.8
Frit Slurry Addition 1	0	0.8
Frit Slurry Addition 2	0	0.4
Frit Slurry Addition 3	0	0.1
<b>Total SME N<sub>2</sub>O Evolution</b>	3.2	6.8

The nitrous oxide masses from the SME cycle could only begin to explain the much larger nitrate losses indicated by the nitrate balance above. Sometimes the sensitivity of the second column on the GC, however, is adjusted in such a manner that small quantities of N<sub>2</sub>O are not integrated and reported. This may have happened in Run SB3A-8 toward the end of the SME cycle. In this case the total evolved mass would be understated.

The SRAT nitrate ion results in the nitrate material balances and the SRAT nitrous oxide generation results were combined to estimate the coefficient for nitrite ion acid demand in the SRAT acid stoichiometry. A first principles calculation for the acid demand for nitrite destruction was made using the data. The calculation assumed no nitrate destruction. It was also assumed that there were no unidentified reaction paths for nitrite destruction beyond those given in WSRC-TR-2003-00041 [9]. The nitrite converted to NO was calculated by Equation 8

$$\text{nitrite reduced to NO} = \text{total nitrite lost} - 2 * \text{N}_2\text{O formed} - 3 * \text{nitrate formed} \quad \text{Eq (8)}$$

where all terms are in moles. This completed the predicted allocation of nitrite destruction among the three identified paths – to nitrate, to NO, and to N<sub>2</sub>O. This allowed a calculation of the total moles of acid demand per mole of nitrite destroyed. Equation 9 was used.

$$\text{Eq (9)} \quad \frac{\text{moles acid used}}{\text{NO}_2^- \text{ lost}} = \frac{4 * \text{N}_2\text{O made}}{\text{NO}_2^- \text{ lost}} + \frac{2 * \text{NO}_3^- \text{ made}}{3 * \text{NO}_2^- \text{ lost}} + \frac{3 * \text{NO}_2^- \text{ reduced to NO}}{2 * \text{NO}_2^- \text{ lost}}$$

The individual results for the two runs are given in the last column of Table 28.

**Table 28 - Calculated SRAT Acid Demand for Nitrite Destruction**

RUN	% nitrite to nitrate (as moles nitrite converted)	% nitrite to N <sub>2</sub> O (moles)	% reduced to NO by HCOOH	total moles acid/mole nitrite lost
SB3A-8	49.5	22.5	28.0	1.20
SB3A-9	0	49.5	50.5	1.75

The individual acid requirements are similar to those obtained in earlier SB3 SRAT simulations.[9,18]

The SB3 simulant acid demands for nitrite destruction from Phase I, Phase II, and two SRAT runs supporting the slurry fed melt rate furnace (SMRF) work are compared to the Tank 8 data [9] in Table 29. The uncertainties for the Decant 5 (69% oxalate), Decant 9 (40% oxalate), and Tank 8 simulant results are the standard deviations associated with averages over two or more runs. The uncertainties for the Decant 7 and extremely washed simulant results, however, are engineering estimates based on some of the uncertainties in the batch data and analytical results. They are consistent with the standard deviations determined for Decant 5 and Decant 9.

**Table 29 - Mean Acid Requirement for Nitrite Destruction vs. Oxalate Content**

Tank 8	Moles Acid per Mole Nitrite	SB3 Phase I, Phase II, & SMRF	Moles Acid per Mole Nitrite
0% Oxalate	1.17 ± 0.09	1% Oxalate – Extremely Washed	0.8 ± 0.3
25% Oxalate	1.52 ± 0.16	40% Oxalate – Decant 9	1.53 ± 0.31
50% Oxalate	1.44 ± 0.14	52% Oxalate – Decant 7	1.1 ± 0.3
75% Oxalate	1.60 ± 0.10	69% Oxalate – Decant 5	1.39 ± 0.29

The value for Decant 5 was averaged over all available runs of Decant 5 simulant with supporting GC data. This included SB3A-1 from Phase I at 10% nominal noble metals. It also included two runs of Decant 5 at 100% nominal noble metals in the 22-L SRAT to make feed for the SMRF. Finally, it included the result for SB3A-8 from Phase II. The value for the 40% oxalate case included SB3A-2 from Phase I at 10% nominal noble metals and SB3A-9 from Phase II. The average results for both Decant 5 and Decant 9 have increased as more data has become available. They now are much closer on average to the Tank 8 simulant results than after Phase I [18]. There was no statistically significant evidence that the nitrite acid requirement actually changed from Tank 8 to SB3 simulant. The one effect that was consistently evident was that the acid demand for nitrite destruction seemed higher in sludges with significant oxalate than without any oxalate.

The current DWPF algorithm factor for nitrite destruction is 0.75 moles acid/mole nitrite. Only runs with minimal oxalate appear to have a demand this small, Table 29. Note that the 4-L and 22-L SRAT rigs reflux through a MWWT. The contents of the MWWT during the SRAT cycle are typically very acidic. This is believed to be very similar to DWPF operation, however mass transfer resistances and mixing times are shorter in the bench-scale equipment. The reintroduction of nitrate or nitrite to the SRAT via the reflux stream could introduce complications into the analysis above. The proposed SB3 acid addition stoichiometry algorithm [4] has a factor of 1.95 moles acid/mole nitrite. This is more than double the current coefficient on nitrite in the Hsu/Marek algorithm used in DWPF. The proposed factor appears to be more consistent with the data for runs with 25-75% of the expected oxalate in Tank 7 than with the data for runs with no oxalate.

The present results for nitrite destruction still suggest that the use of constant coefficients in the acid calculation stoichiometry algorithm will at best give an approximation to the actual acid requirement. It may be that a different coefficient is optimal for every sludge processed. It is possible that the noble metal concentrations also effect the acid requirement for nitrite destruction by selectively altering the preferred reaction paths.

## 7.0 CONCLUSIONS

The two SRAT/SME runs with SB3 simulant and the nominal noble metals at excess acid levels were completed. The SB3 compositions tested included Decant 5 (69% remaining sodium oxalate after washing/decanting) and Decant 9 (40% remaining sodium oxalate after washing/decanting). The proposed acid addition equation was tested in these runs and successfully destroyed nitrite present to below the DWPF limit. However, at the excess acid level tested, the DWPF hydrogen generation limit in the SRAT was exceeded in one run (Decant 5 or Run SB3A-8) and was approached in the other (Decant 9 or Run SB3A-9). The Phase II runs were performed with ~25% more acid than the amount used in the Phase I runs. The data suggest that an upper limit on the acid addition amount would have to be implemented if the composition to be processed in DWPF was similar to the decant scenarios tested and contained the projected levels of noble metals. This limit would best be placed on the amount of formic acid since its addition primarily drives the hydrogen generation; however, by doing this a redox target other than 0.200 may have to be used. No processing problems such as foaming, loss of heat transfer, or air entrainment were seen. As with other SB3 simulant chemical process cell studies, sodium oxalate continued to have an impact on the acid addition required and the reactions that are occurring during processing.

## 8.0 PATH FORWARD

Phase I identified acid addition strategies for Decants 5, 7, and 9, and an extremely washed SB3 simulant at 10% of the nominal level of noble metals. The SB3 defined acid addition equation, along with the projected SB3 redox equation, were tested in Phase II of the simulant flowsheet runs along with preliminary estimates of the upper acid bound. Phase II provided some insight on the upper acid bounds for Decants 5 and 9 with nominal noble metals levels. These same acid addition levels with 10% of the nominal noble metals would not have presented a hydrogen problem based on historical data.

Once the data from the final Tank 7 sample is combined with the Tank 51 heel composition and the other Tank 7 data, it will be combined with the proposed washing and blending strategy. The composition will be evaluated and a decision will be made as to whether the SB3 SRAT/SME testing has adequately bounded the expected composition. Additional runs will be performed as necessary to identify processing parameters for the Tank 51 qualification sample and for the potential blend of SB3 with SB2. Bounding levels of acid will also be defined as necessary for these scenarios.

Mercury reduction was not characterized in these runs because the anticipated Hg content was already below the DWPF limit. The final Tank 7 sample and the Tank 51 Waste Qualification sample results will be evaluated to ensure that the proper level of mercury has been tested. Mercury in the SRAT product will then be characterized as part of that phase of testing to ensure acceptability.

Preliminary rheology data from both phases of testing indicated that the SRAT products for the Decant 5 sludge composition were Newtonian in nature, while the SRAT products for the Decant 9 sludge composition exhibited non-Newtonian behavior. SME product results were questionable from Phase II because of suspected problems with settling during the rheological characterization. As any additional testing is performed to support SB3 qualification and/or the processing of SB2 with SB3, the rheological behavior of the SRAT and SME products will be further investigated. After the completion of the testing, the data will be documented and a report will be issued.

Some problems still exist with the analyses of oxalate in the sludge slurry. Based on the Tank 7 analyses, it appears that oxalate will not be a major contributor to SB3 and will not likely have to be analyzed in the DWPF. However, if the oxalate method is to be implemented in DWPF, more work on the method development may be necessary and the Mobile Lab will have to work with ADS to resolve some of the outstanding issues.

## 9.0 REFERENCES

- [1] C.C. Herman, D.C. Koopman, D.R. Best, and M.F. Williams, “**Sludge Batch 3 Simulant Flowsheet Studies: Phase I SRAT Results**”, WSRC-TR-2003-00088, March 20, 2003, Westinghouse Savannah River Company, Aiken, South Carolina.
- [2] M.A. Rios-Armstrong, **Sludge Batch 3 Flowsheet Studies**, HLW/DWPF/TTR-02-0016, October 30, 2002, Westinghouse Savannah River Company, Aiken, South Carolina.
- [3] C.C. Herman, “**Task Technical & QA Plan: Sludge Batch 3 Simulant Flowsheet Studies**”, WSRC-RP-2002-00563, November 8, 2002, Westinghouse Savannah River Company, Aiken, South Carolina.
- [4] D.C. Koopman, C.M. Jantzen, and T.B. Edwards, “**Acid Addition Stoichiometry for Sludge Batch 3 Processing in the Defense Waste Processing Facility**”, WSRC-TR-2003-00118, February 27, 2003, Westinghouse Savannah River Company, Aiken, South Carolina.
- [5] C.M. Jantzen, J.R. Zamecnik, D.C. Koopman, C.C. Herman, and J.B. Pickett, “**Electron Equivalents Model for Controlling Reduction-Oxidation (Redox) Equilibrium during High Level Waste (HLW) Vitrification**”, WSRC-TR-2003-00126, Westinghouse Savannah River Company, Aiken, South Carolina.
- [6] D.K. Peeler, N.E. Bibler, and T.B. Edwards, “**An Assessment of the Impacts of Adding Am/Cm and Pu/Gd Waste Streams to Sludge Batch 3 (SB3) on DWPF H<sub>2</sub> Generation Rates and Glass Properties**”, WSRC-TR-2002-00145, March 22, 2002, Westinghouse Savannah River Company, Aiken, South Carolina.
- [7] N.E. Bibler, “**Elemental Weight Percent in First and Second Tank 7 Dry Slurry Samples**”, SRT-ITB-2003-00006, January 25, 2003, Westinghouse Savannah River Company, Aiken, South Carolina.
- [8] A.Q. Goslen, “**Estimated Sodium Oxalate in the Tank Farm**”, March 22, 1984, Westinghouse Savannah River Company, Aiken, South Carolina.
- [9] D.C. Koopman, C.C. Herman, and N.E. Bibler, “**Sludge Batch 3 Preliminary Acid Requirement Studies with Tank 8 Simulant**”, WSRC-TR-2003-00041, January 31, 2003, Westinghouse Savannah River Company, Aiken, South Carolina.
- [10] C.C. Herman, D.R. Best, D.C. Koopman, and M.F. Williams, “**Data Summary from SRAT Runs SB3-19 to SB3-24 to Evaluate Sodium Oxalate Addition Levels and SME Processing**”, SRT-GPD-2002-00200, January 27, 2003, Westinghouse Savannah River Company, Aiken, South Carolina.
- [11] D.C. Koopman, “**Run SB3A-8, Phase II Decant 5 Test for Hydrogen Limitation**”, SRT-GPD-2003-00011, February 18, 2003, Westinghouse Savannah River Company, Aiken, South Carolina.
- [12] D.C. Koopman, “**Run SB3A-9, Phase II Decant 9 Test for Hydrogen Limitation**”, SRT-GPD-2003-00012, February 18, 2003, Westinghouse Savannah River Company, Aiken, South Carolina.
- [13] L27 Manual, ITS/TNX Procedures Manual, 2002.
- [14] C.C. Herman, “**Analytical Study Plan: Sludge Batch 3 Simulant Flowsheet Studies**”, WSRC-RP-2002-00577, November 12, 2002, Westinghouse Savannah River Company, Aiken, South Carolina.
- [15] C.C. Herman, D.R. Best, T.B. Edwards, J.G. George, D.C. Koopman, and M.F. Williams, “**Data Summary from Sludge Batch 3 Simulant SRAT Runs to Evaluate Impacts of Noble Metals Mass and Coal Size, Mass, and Treatment**”, SRT-GPD-2002-00121, November 1, 2002, Westinghouse Savannah River Company, Aiken, South Carolina.

- [16] C.C. Herman, D.C. Koopman, N.E. Bibler, D.R. Best, and M.F. Williams, “**SRAT Processing of Sludge Batch 3 Simulant to Evaluate Impacts of H-Canyon Slurry Containing Precipitated Pu and Gd**”, WSRC-TR-2002-00322, July 25, 2002, Westinghouse Savannah River Company, Aiken, South Carolina.
- [17] D.C. Koopman and C.C. Herman, “**Analysis of Initial Sludge Batch 3 Slurry Mix Evaporator Simulations**”, SRTC-GPD-2003-00019, March 3, 2003, Westinghouse Savannah River Company, Aiken, South Carolina.
- [18] D.C. Koopman, C.C. Herman, and N.E. Bibler, “**Sludge Batch 3 Preliminary Acid Requirement Studies with Simulants**”, WSRC-TR-2003-00132, February 27, 2003, Westinghouse Savannah River Company, Aiken, South Carolina.

## 10.0 ACKNOWLEDGMENTS

The authors would like to acknowledge the following personnel and groups for their assistance in performing the studies and analyzing the required samples:

- S.O. King, J.W. Duvall, V.J. Williams, and T.O. Burckhalter for performing the SRAT runs.
- P.A. Toole, M.L. Moss, J. Jansen, and J.G. Wheeler for providing assistance with the analyses.
- A. Ekechukwu and ADS for providing analytical support.
- E.K. Hansen and D.M. Marsh for performing rheology analyses.

**Appendix A – SRAT/SME Run Parameters**

Table A - 1: SRAT/SME Run Parameters

Parameter	SB3A-8	SB3A-9
Decant #/% Oxalate Remaining	5 / 69%	9 / 40%
Measured Sludge Hydroxide Equivalents @pH=7, M	0.371	0.416
Total Inorganic Carbon, ug/ml	1210	1150
Sand Content (grams added)	3.923	5.455
Coal Content (grams added)	2.493	3.467
Hg Content (grams added)	0.269	0.373
Ag Content (grams added)	0.0022	0.0027
Pd Content (grams added)	0.097	0.135
Rh Content (grams added)	0.179	0.249
Ru Content (grams added)	0.643	.894
Rinse Water for Trim Chemicals (g)	157.90	111.91
Sludge Slurry Mass Trimmed to Match Decant (g)	2912.1	2907.0
Total Feed with Trim Chemicals (g)	2925.0	2924.9
Starting SRAT Feed Amount with Rinse Water (g) <sup>1</sup>	2948.6	2905.0
DWPF Scale Factor	9165	9165
Acid Stoichiometry	125%	135%
Nitric Acid Amount Added (ml) - 10.25 molar Nitric Acid	129.63	96.54
Nitric Acid Addition Rate (ml/min)	0.84	0.84
Nitric Acid Moles	1.329	0.989
Formic Acid Amount Added (ml) - 23.22 molar Formic Acid	106.98	97.33
Formic Acid Addition Rate (ml/min)	0.83	0.84
Formic Acid Moles	2.484	2.260
SRAT Dewater Amount (g)	428.2	348.3
Condensing/Dewater Time during SRAT (hrs)	1.5	1.8
Total SRAT Time at Boiling (hrs)	12	13.8
SRAT Target Boil-up Rate (g/min)	4.12	4.12
SRAT Air Purge on System (slm)	0.580	0.580
SRAT Helium Purge on System (sccm)	2.90	2.90
Initial Sludge pH with Trim Chemicals	11.43	12.13
Minimum pH during SRAT	4.33	4.58
pH at End of SRAT (at boiling)	7.15	7.40
SME Air Purge (sccm)	203	203
SME He Purge (sccm)	1.02	1.02
SME Target Boil-up Rate (g/min)	3.60	3.60
Decon Canister Addition Mass (g)	430	430
Decon Canister Water Addition Rate (ml/min)	43	43
Decon Canister #1 Condensing/Dewater Time (hrs)	2.12	2.10
Decon Canister #2 Condensing/Dewater Time (hrs)	2.00	2.42
Decon Canister #3 Condensing/Dewater Time (hrs)	2.00	2.18
Decon Canister #4 Condensing/Dewater Time (hrs)	1.75	2.50
Decon Canister #5 Condensing/Dewater Time (hrs)	1.62	2.00
Waste Loading Target	35 wt%	35 wt%
Frit Type	202	202
SME Frit Addition Mass (g) - 3 Additions	181.52	200.28
Frit Addition Water (g) 3 additions	173.50	196.94
Frit Addition Formic Acid (g) 3 additions	3.02	3.34
SME Frit Dewater Target Amount (g)	471.7	451.3
First Frit Condensing/Dewater Time (hrs)	1.92	2.03
Second Frit Condensing/Dewater Time (hrs)	1.97	2.68
Third Frit Condensing/Dewater Time (hrs)	2.00	1.75
Minimum pH during SME Run	7.03	7.20
Final SME Product pH (at boiling)	7.56	7.69

<sup>1</sup>Reflects the starting mass after the initial samples were removed for analyses.

Table A - 2: SRAT/SME Operating Data and Mass Balance

SB3A-8	Time	Mass Change (g)	Comments	Running Mass Balance (g)
Sludge, Trim Chemicals, & Flush Water	16:30	3082.9088	107.9 g extra water needed to rinse	3082.91
SB3A-8 SLUDGE	19:22	134.3		2948.61
Started heating	7:45			
Added 1:10 Antifoam & Water	8:25	11.2	5.6 g of each	2959.81
Started Nitric Acid	9:14			
Stopped Nitric Acid	10:55	109.8	He problem so cycle stopped, 84.03 ml added	3069.64
Started reheating and GC	19:20			
Restarted Nitric Acid	19:45			
Finished Nitric Acid	20:41	59.85	Total nitric acid 129.82 ml	3129.48
SB3A-8 SRAT-IC-A	20:46	11.84		3117.64
Started Formic Acid	20:49			
SB3A-8 SRAT-IC-B	22:10	13.73		3103.91
Finished Formic Acid	22:59	128.6	Total formic acid 106.9 ml	3232.51
SB3A-8 SRAT-IC-0	23:00	13.05		3219.46
SB3A-8 SRAT-IC/ICP-0	23:02	11.77		3207.69
Added 1:10 Antifoam & Water	23:20	22.4	11.2 g of each	3230.09
Boiling Started	23:28			
SB3A-8 SRAT-IC-1	23:58	12.72		3091.37
Dewater finished	0:56	428.2		2789.17
SB3A-8 SRAT-IC-2	1:00	12.92		2776.25
SB3A-8 SRAT-IC-4	3:00	11.99		2764.26
SB3A-8 SRAT-IC-6	5:00	11.77		2752.49
SB3A-8 SRAT-IC-8	7:00	12.31		2740.18
SB3A-8 SRAT-IC-10	9:00	12.73		2727.45
SB3A-8 SRAT-IC-12	11:00	12.08		2715.37
SB3A-8 SRAT-IC-14	11:28	11.79		2703.58
SRAT complete	11:28	2570	Est. SRAT Product mass – Considers FAVC & estimated 3% of initial sludge mass loss	
SB3A-8 SRAT-FAVC-1	11:36	44.78		2658.80
SB3A-8 SRAT-Product-1	11:45	104.78		2554.02
SB3A-8 SRAT-Product-2	11:50	110.17		2443.85
Added 1:10 Antifoam & Water	12:05	5.6	2.8 g of each	2449.45
Completed 1st Canister Addition	12:44	430		2879.45
Started 1st Canister Dewater	13:00			
Completed 1st Canister Dewater	15:13	430		2449.45
Completed 2nd Canister Addition	15:32	430		2879.45
Started 2nd Canister Dewater	15:52			
Completed 2nd Canister Dewater	17:52	430.1		2449.35
Completed 3rd Canister Addition	18:15	430		2879.35
Started 3rd Canister Dewater	18:34			
Completed 3rd Canister Dewater	20:24	430		2449.35
Completed 4th Canister Addition	20:41	430		2879.35
Started 4th Canister Dewater	20:52			
Completed 4th Canister Dewater	22:37	430		2449.35
Completed 5th Canister Addition	22:57	430		2879.35
Started 5th Canister Dewater	23:07			
Completed 5th Canister Dewater	0:44	430.1		2449.25
SB3A-8 SME-IC-0	0:47	12.90		2436.35
1st Frit Addition	1:00	181.52		2617.87
1st Formic Addition	1:00	3.03		2620.90
1st Frit Water Addition	1:00	173.5		2794.40
1st Frit Dewater Started	1:17			
1st Frit Dewater Complete	3:12	471.7		2322.70
2nd Frit Addition	3:26	181.52		2504.22

SB3A-8	Time	Mass Change (g)	Comments	Running Mass Balance (g)
2nd Formic Addition	3:26	3.03		2507.25
2nd Frit Water Addition	3:26	173.5		2680.75
2nd Frit Dewater Started	3:38			
2nd Frit Dewater Complete	5:36	471.7		2209.05
3rd Frit Addition	5:46	181.52		2390.57
3rd Formic Addition	5:46	3.03		2393.60
3rd Frit Water Addition	5:46	173.5		2567.10
3rd Frit Dewater Started	6:05			
3rd Frit Dewater Complete	8:05	471.7		2095.40
SME Complete/Final product	8:05	1922	Delta	173.40
SB3A-8 SME-FAVC-1		4.7	Delta'	187.98
SB3A-8 SME-MWWT-1	10:41	10.05	171.2 g initial, 151.92 g final	

Delta is the difference between the actual weight and the predicted weight.

Delta' takes in the difference in the actual and predicted weights including material lost to the FAVC and MWWT.

Table A - 2: SRAT/SME Operating Data and Mass Balance (Continued)

SB3A-9	Time	Mass Change (g)	Comments	Running Mass Balance (g)
Sludge, Trim Chemicals, & Flush Water	6:10	3036.8336	61.9 g extra water needed for rinsing	3036.83
SB3A-9 SLUDGE	7:00	131.8		2905.03
Started heating	7:45			
Added 1:10 Antifoam & Water	8:00	11.2	5.6 g of each	2916.23
Started Nitric Acid	8:51			
Stopped Nitric Acid	9:08		Temp-O-Trol problem	
Restarted Nitric Acid	9:24			
Stopped Nitric Acid	9:42		Temp-O-Trol problem	
Restarted Nitric Acid	10:28			
Finished Nitric Acid	11:48	126.3	Total nitric acid 96.605 ml	3042.50
SB3A-9 SRAT-IC-A	11:51	11.52		3030.98
Started Formic Acid	12:03			
Stopped Formic Acid	12:21		pH probe problem	
Restarted Formic Acid	12:27		pH probe changed	
SB3A-9 SRAT-IC-B	13:30	12.33		3018.65
Finished Formic Acid	14:05	116.8	Total formic acid 97.337 ml	3135.45
SB3A-9 SRAT-IC-0	14:08	12.45		3123.00
SB3A-9 SRAT-IC/ICP-0	14:13	11.42		3111.58
Added 1:10 Antifoam & Water	14:17	22.4	11.2 g of each	3133.98
Boiling Started	14:35			
SB3A-9 SRAT-IC-1	15:05	11.38		3038.60
Dewater finished	16:23	340.3		2782.30
SB3A-9 SRAT-IC-2	16:50	11.49	Air cylinder problem	2770.81
SB3A-9 SRAT-IC-4	18:23	13.36		2757.45
SB3A-9 SRAT-IC-6	20:23	12.74		2744.71
SB3A-9 SRAT-IC-8	22:23	13.07		2731.64
SB3A-9 SRAT-IC-10	0:23	12.61		2719.03
SB3A-9 SRAT-IC-12	2:23	12.72		2706.31
SB3A-9 SRAT-IC-14	4:23	11.26		2695.05
SRAT complete	4:23	2598	Estimated SRAT Product with FAVC loss and assumed 3% initial slurry mass loss.	
SB3A-9 SRAT-FAVC-1	4:41	10.08		2684.97
SB3A-9 SRAT-Product-1	4:37	112.72		2572.25
SB3A-9 SRAT-Product-2	4:39	113.26		2458.99
Added 1:10 Antifoam & Water	4:55	5.6	2.8 g of each	2464.59
Completed 1st Canister Addition	5:06	430		2894.59
Started 1st Canister Dewater	6:40			
Completed 1st Canister Dewater	8:46	430		2464.59
Completed 2nd Canister Addition	9:10	430		2894.59
Started 2nd Canister Dewater	9:35			
Completed 2nd Canister Dewater	12:00	430		2464.59
Completed 3rd Canister Addition	12:28	430		2894.59
Started 3rd Canister Dewater	12:54			
Completed 3rd Canister Dewater	15:05	430		2464.59
Completed 4th Canister Addition	15:32	430		2894.59
Started 4th Canister Dewater	15:56			
Completed 4th Canister Dewater	19:24	430		2464.59
Completed 5th Canister Addition	19:40	430		2894.59
Started 5th Canister Dewater	?			
Completed 5th Canister Dewater	21:00	430		2464.59
SB3A-9 SME-IC-0	21:13	12.07		2452.52
1st Frit Addition	21:23	200.28		2652.80
1st Formic Addition	21:23	3.34		2656.14
1st Frit Water Addition	21:23	196.94		2853.08

SB3A-9	Time	Mass Change (g)	Comments	Running Mass Balance (g)
1st Frit Dewater Started	21:55			
1st Frit Dewater Complete	23:57	451.3		2401.78
2nd Frit Addition	23:58	200.28		2602.06
2nd Formic Addition	23:58	3.34		2605.40
2nd Frit Water Addition	23:58	196.94		2802.34
2nd Frit Dewater Started	0:07			
2nd Frit Dewater Complete	2:48	451.3		2351.04
3rd Frit Addition	3:07	200.28		2551.32
3rd Formic Addition	3:07	3.34		2554.66
3rd Frit Water Addition	3:07	196.94		2751.60
3rd Frit Dewater Started	3:49			
3rd Frit Dewater Complete	5:34	451.3		2300.30
SME Complete/Final product		2073.2	Delta	227.10
SB3A-9 SME-FAVC-1	9:32	4.18	Delta'	231.85
SB3A-9 SME-MWWT-1	9:25	10.21	Initial 172.9 g, final 173.9 g	

Delta is the difference between the actual weight and the predicted weight.

Delta' takes in the difference in the actual and predicted weights including material lost to the FAVC and MWWT.